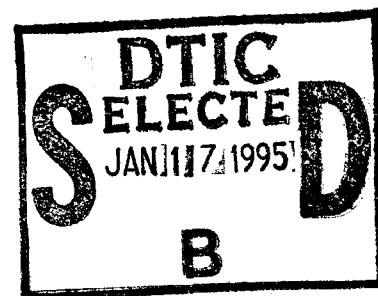


TECHNICAL REPORT RD-SS-94-18

THIN-FILM RESISTOR ARRAY CHARACTERIZATION

Vicki Vanderford  
Scott Mobley  
Systems Simulation and Development Directorate  
Research, Development, and Engineering Center

December 1994



U. S. ARMY MISSILE COMMAND

**Redstone Arsenal, Alabama** 35898-5000

*Approved for public release; distribution is unlimited.*

DTIC QUALITY INSPECTED

19950113 022

## **DESTRUCTION NOTICE**

**FOR CLASSIFIED DOCUMENTS, FOLLOW THE PROCEDURES IN DoD 5200.22-M, INDUSTRIAL SECURITY MANUAL, SECTION II-19 OR DoD 5200.1-R, INFORMATION SECURITY PROGRAM REGULATION, CHAPTER IX. FOR UNCLASSIFIED, LIMITED DOCUMENTS, DESTROY BY ANY METHOD THAT WILL PREVENT DISCLOSURE OF CONTENTS OR RECONSTRUCTION OF THE DOCUMENT.**

## **DISCLAIMER**

**THE FINDINGS IN THIS REPORT ARE NOT TO BE CONSTRUED AS AN OFFICIAL DEPARTMENT OF THE ARMY POSITION UNLESS SO DESIGNATED BY OTHER AUTHORIZED DOCUMENTS.**

## **TRADE NAMES**

**USE OF TRADE NAMES OR MANUFACTURERS IN THIS REPORT DOES NOT CONSTITUTE AN OFFICIAL ENDORSEMENT OR APPROVAL OF THE USE OF SUCH COMMERCIAL HARDWARE OR SOFTWARE.**

UNCLASSIFIED

SECURITY CLASSIFICATION OF THIS PAGE

## REPORT DOCUMENTATION PAGE

Form Approved  
OMB No. 0704-0188  
Exp. Date: Jun 30, 1986

1a. REPORT SECURITY CLASSIFICATION UNCLASSIFIED			1b. RESTRICTIVE MARKINGS									
2a. SECURITY CLASSIFICATION AUTHORITY			3. DISTRIBUTION/AVAILABILITY OF REPORT Approved for public release; distribution is unlimited.									
2b. DECLASSIFICATION/DOWNGRADING SCHEDULE												
4. PERFORMING ORGANIZATION REPORT NUMBER(S) TR-RD-SS-94-18			5. MONITORING ORGANIZATION REPORT NUMBER(S)									
6a. NAME OF PERFORMING ORGANIZATION Sys. Sim. and Dev. Dir. RD&E Center		6b. OFFICE SYMBOL (If applicable) AMSMI-RD-SS-HW	7a. NAME OF MONITORING ORGANIZATION									
6c. ADDRESS (City, State, and ZIP Code) Commander, U. S. Army Missile Command ATTN: AMSMI-RD-SS-HW Redstone Arsenal, AL 35898-5252			7b. ADDRESS (City, State, and ZIP Code)									
8a. NAME OF FUNDING / SPONSORING ORGANIZATION		8b. OFFICE SYMBOL (If applicable)	9. PROCUREMENT INSTRUMENT IDENTIFICATION NUMBER									
8c. ADDRESS (City, State, and ZIP Code)			10. SOURCE OF FUNDING NUMBERS									
			<table border="1"> <tr> <td>PROGRAM ELEMENT NO.</td> <td>PROJECT NO.</td> <td>TASK NO.</td> <td>WORK UNIT ACCESSION NO.</td> </tr> <tr> <td></td> <td></td> <td></td> <td></td> </tr> </table>		PROGRAM ELEMENT NO.	PROJECT NO.	TASK NO.	WORK UNIT ACCESSION NO.				
PROGRAM ELEMENT NO.	PROJECT NO.	TASK NO.	WORK UNIT ACCESSION NO.									
11. TITLE (Include Security Classification) Thin-Film Resistor Array Characterization												
12. PERSONAL AUTHOR(S) Vicki Vanderford and Scott Mobley												
13a. TYPE OF REPORT Final		13b. TIME COVERED FROM Jan 94 to Jun 94	14. DATE OF REPORT (Year, Month, Day) December 1994	15. PAGE COUNT 75								
16. SUPPLEMENTARY NOTATION												
17. COSATI CODES			18. SUBJECT TERMS (Continue on reverse if necessary and identify by block number)									
FIELD	GROUP	SUB-GROUP										
			Hardware-in-the-Loop (HWIL), Thin-Film Resistor Array									
			Infrared Scene Projector (IRSP), Spatial Uniformity									
			Dynamic Range, Temporal Response									
19. ABSTRACT (Continue on reverse if necessary and identify by block number) This paper provides the results of thin-film resistor array testing which was recently performed at the System Simulation and Development Directorate (SS&DD), Research, Development, and Engineering Center (RDEC). The objective of these tests was to determine the suitability of the Australian thin-film resistor technology for use as a key component in an Infrared Scene Projector (IRSP) for Hardware-in-the-Loop (HWIL) simulations involving systems which utilize linear rows of detectors. The tests were configured to measure spatial uniformity, temporal response, dynamic range, and relative energy output as a function of power input. D650 funding was used to purchase the resistor arrays.												
20. DISTRIBUTION/AVAILABILITY OF ABSTRACT <input type="checkbox"/> UNCLASSIFIED/UNLIMITED <input checked="" type="checkbox"/> SAME AS RPT. <input type="checkbox"/> DTIC USERS			21. ABSTRACT SECURITY CLASSIFICATION UNCLASSIFIED									
22a. NAME OF RESPONSIBLE INDIVIDUAL Vicki Vanderford			22b. TELEPHONE (Include Area Code) (205) 955-7326	22c. OFFICE SYMBOL AMSMI-RD-SS-HW								

DTIC QUALITY INSPECTED 3

DD FORM 1473, 84 MAR

83 APR edition may be used until exhausted.  
All other editions are obsolete.SECURITY CLASSIFICATION OF THIS PAGE  
UNCLASSIFIED

## ACKNOWLEDGEMENT

A special thanks to Ms. Charlene Coke of the Foreign Intelligence Division, Intelligence and Security Directorate, U. S. Army Missile Command, for her cooperation and support of the work reported herein.

<b>Accession For</b>	
NTIS GRA&I	<input checked="checked" type="checkbox"/>
DTIC TAB	<input type="checkbox"/>
Unannounced	<input type="checkbox"/>
Justification	
By	
Distribution	
Availability Codes	
Dist	Avail and/or Special
A-1	

## TABLE OF CONTENTS

	<u>Page</u>
I. INTRODUCTION .....	1
II. RESISTOR ARRAY TECHNOLOGY .....	2
III. AUSTRALIAN RESISTOR ARRAY PHYSICAL CHARACTERISTICS .	6
IV. MEASUREMENT METHODS .....	7
V. SUMMARY .....	8
REFERENCES .....	13
APPENDIX A: TEST DATA .....	A-1
APPENDIX B: DELIVERED TEST DATA .....	B-1

## LIST OF ILLUSTRATIONS

<u>Figure</u>	<u>Title</u>	<u>Page</u>
1.	Resistor Bridge Example .....	3
2.	Thin-Film Resistor Example .....	4
3.	Honeywell Suspended Membrane Resistor Example .....	5
4.	British Aerospace Suspended Membrane Resistor .....	5
5.	Australian Resistor .....	6
6.	Output Versus Power Test Setup .....	9
7.	3 to 5 Microns, Substrate at 77 K .....	9
8.	3 to 5 Microns, Substrate at Ambient Temperature .....	10
9.	8 to 12 Microns, Substrate at 77 K .....	10
10.	8 to 12 Microns, Substrate at Ambient Temperature .....	11
11.	Temporal Response Test Setup .....	11
12.	Example Curve of Rise and Fall Time for a Step Input .....	12

## I. INTRODUCTION

Approximately five years ago, the Systems Simulation and Development Directorate (SS&DD) was tasked with the development of a Hardware-in-the-Loop (HWIL) simulator to support the development of the Sense And Destroy ARmor Munition (SADARM). This effort required the implementation of a simulation facility which could provide simultaneous "inband" stimulation of the munition's Millimeter Wave (MMW) and Infrared (IR) sensors. Because SADARM was not a guided missile and, therefore, had no guidance loop to close, it was determined that the easiest approach would be to strap the seeker hardware down and to basically spin the world in front of the unit under test. Although this approach minimized several problems, it created one which could not be readily overcome. Mainly, the requirement to spin the world forced the IR projector to be extremely fast (i.e., temporal frame rate 5000 Hz) to accurately simulate the effect of the rising and falling edge of a target when scanned across by the SADARM seeker. However, it minimized the resolution requirements placed on the IR projector which was probably more of a problem. Accordingly, the required operational IR projector would ideally support a frame rate of 5000 Hz and would have at least a 2 x 32 element resolution.

The initial approach taken by SS&DD was to develop a resistor array with the identified characteristics. This led to the purchase of two such devices at an approximate cost of \$500K. These delivered arrays had many problems and had difficulty meeting the temporal responses required for the strap down test configuration. In addition, the arrays were unreliable and proved almost impossible to calibrate adequately. Attempts to purchase additional arrays from the same vendor proved difficult and if possible at all would have been very expensive. Given the problems which were experienced and the realization that another approach was required, SS&DD began to consider other options approximately three years ago. These options included the purchase of similar devices from an Australian company which was supporting the Australian Defence Science and Technology Organization (DSTO) or the development of a novel IR laser diode projector which appeared capable of meeting the specifications, but was unproven and, accordingly, had a high risk. D650 funding was provided to acquire the Australian resistor arrays; therefore, it was possible for SS&DD to take both routes for the development of an IR projector for HWIL simulation support of the SADARM system.

This report provides a description of the test data taken on one of the four Australian arrays which were received on 23 December 1993. Similar data could be easily obtained on the remaining three devices, but because of the finite lifetime associated with the resistor elements it was determined that it would be better to limit the number of cycles on the devices at this time. An assessment of the utility of the devices for inclusion in a HWIL simulation or for other sensor testing is also provided. A complete copy of the raw test data is provided in Appendix A for those interested in the exact performance figures of merit which were achieved by the devices tested.

## II. RESISTOR ARRAY TECHNOLOGY

Before continuing with the discussion of the Australian array's performance, a brief discussion of general resistor array operation and the various methods for their fabrication is provided. The basic operational principle of the resistor arrays is relatively simple. Electric current is passed through the individual resistor elements which heat up and emit IR energy in accordance with Planck's law. The amount of energy produced is dependent on the resistor temperature, the ratio of active to total pixel area (i.e. fill factor) and emissivity. Three distinct types of devices are currently under development in the United States, United Kingdom, and Australia. These are the silicon bridge resistor, the thin-film resistor, and the suspended membrane resistor. When configured as large Two-Dimensional (2-D) arrays (i.e., resolutions of  $128^2$  and greater), the resistors of either approach are generally addressed a line at a time through a multiplexed transistor drive network. This multiplexed approach uses the gate capacitance of the transistor to maintain a voltage across the resistor until it is readdressed thus minimizing the resultant flicker. The devices tested had a resolution of  $2 \times 36$  elements. Given the few number of resistor elements (i.e., 72), a simple drive circuit where each resistor element had a direct connection was all that was required.

The resistor bridge devices consist of a silicon resistor element suspended over an etched cavity. The cavity backed devices are monolithic in construction and are fabricated on standard silicon wafers. They typically have very small active areas and poor emissivity characteristics. Resistor temperatures of 1000 K have been demonstrated. However, fill factors less than 10 percent and emissivities less than 0.20 degrade the effective temperature performance substantially. The bridge elements are small and frame rates on the order of 400 Hz are readily achievable when the substrate is cooled. Crosstalk between adjacent resistors is minimal because of the thermally isolated cavity structure of the resistor. Arrays of  $128 \times 128$  elements have been fabricated and have been integrated into a projection system. Tests of the prototype system have been performed and have largely validated previous assessments that the device would yield minimal effective temperatures and, as a result, an extremely low dynamic range. The fabrication of larger structures is possible, but yield problems could limit the development of arrays larger than  $256 \times 256$ . Figure 1 shows an example of the typical resistor bridge structure.

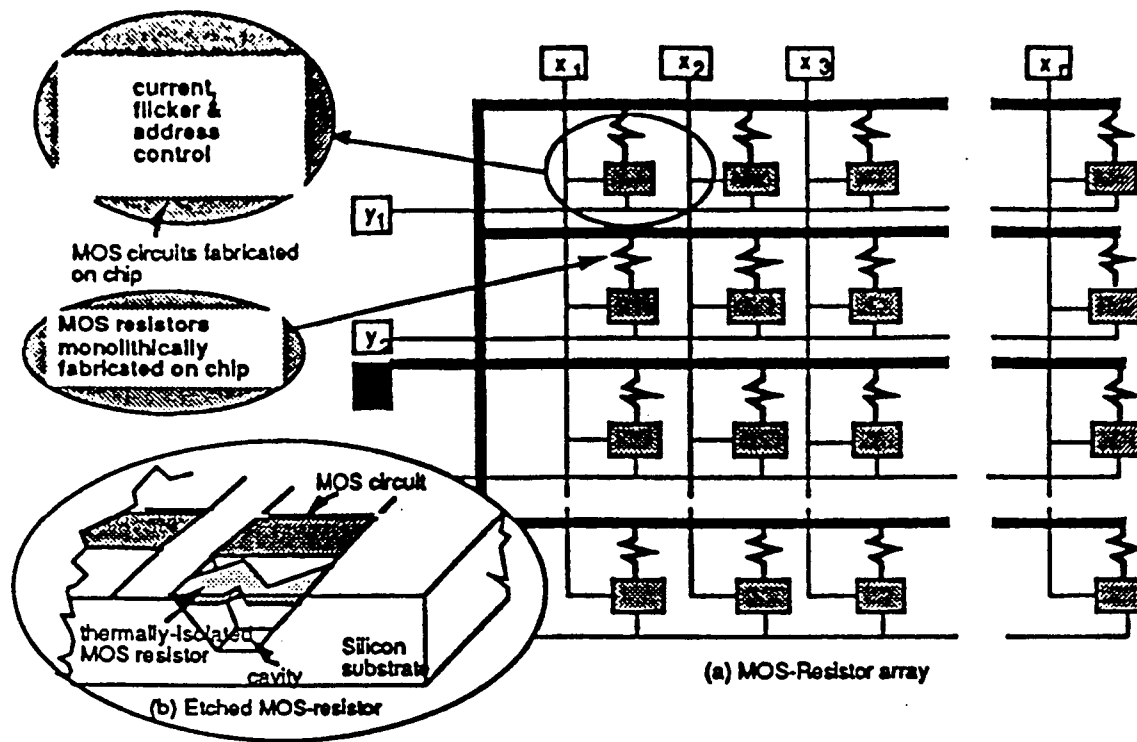
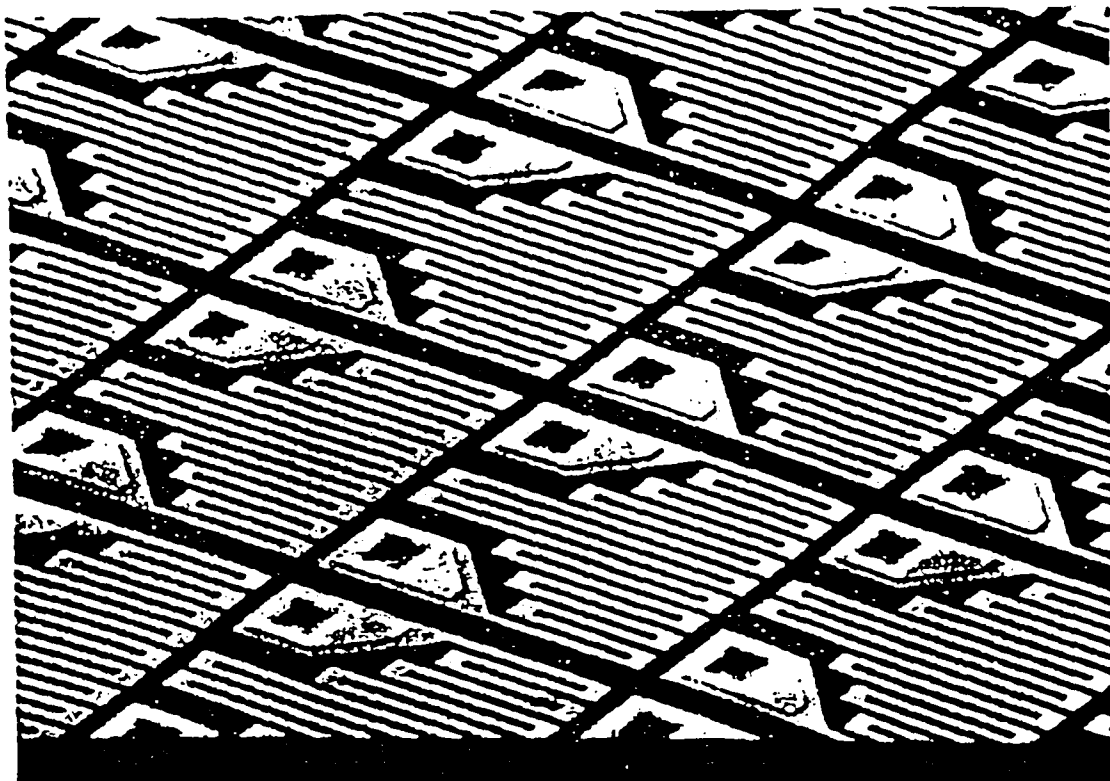


Figure 1. Resistor Bridge Example

Until recently, the isolated thin-film resistor approach was by far the most popular technology for IR projector applications. Arrays based on this have been developed by several companies. In contrast to the seemingly straight forward fabrication process of the cavity backed devices, the fabrication of these structures is very complex and requires several hundred additional processing steps which has functioned to reduce yields even further. Resistor temperatures of 700 K have been demonstrated. The fill factor and emissivity characteristics are substantially better than those with the cavity backed devices. Fill factors on the order of 50 percent and emissivities of 0.50 have been achieved. Accordingly, the effective temperature generated by the pixel will be substantially less than the active resistor temperature. The structure of these devices yields a longer time constant and a frame rate which is limited to the 30 to 60 Hz range. Because the resistors are not completely isolated from adjacent components in the array crosstalk will be evident in any simulated scene. Cooling of the substrate also presents a difficult problem which must be considered in any projector design using this technology. Arrays of  $256^2$  elements have been fabricated. Because of yield limitations, it appears that the production of larger arrays is unlikely. An example of this approach is provided in Figure 2.



*Figure 2. Thin-Film Resistor Example*

The development of the suspended resistor arrays has proceeded at a relatively fast pace with two different approaches being well documented in the literature. Figures 3 and 4 provide a schematic of each approach. From the figure, it is apparent that the two concepts are very similar in architecture and visual appearance. Both utilize a two level construction where a serpentine resistor element is supported over a substrate on which the drive electronics are etched. Maximum fill factors of 90 percent and maximum frame rates of several hundred hertz have been demonstrated in prototype devices. Pixels ranging in size from 50 micron x 50 micron to 100 micron x 100 micron have been constructed. Although these improvements over the other technologies should improve overall performance substantially, no test data has been taken to completely verify this assumption.

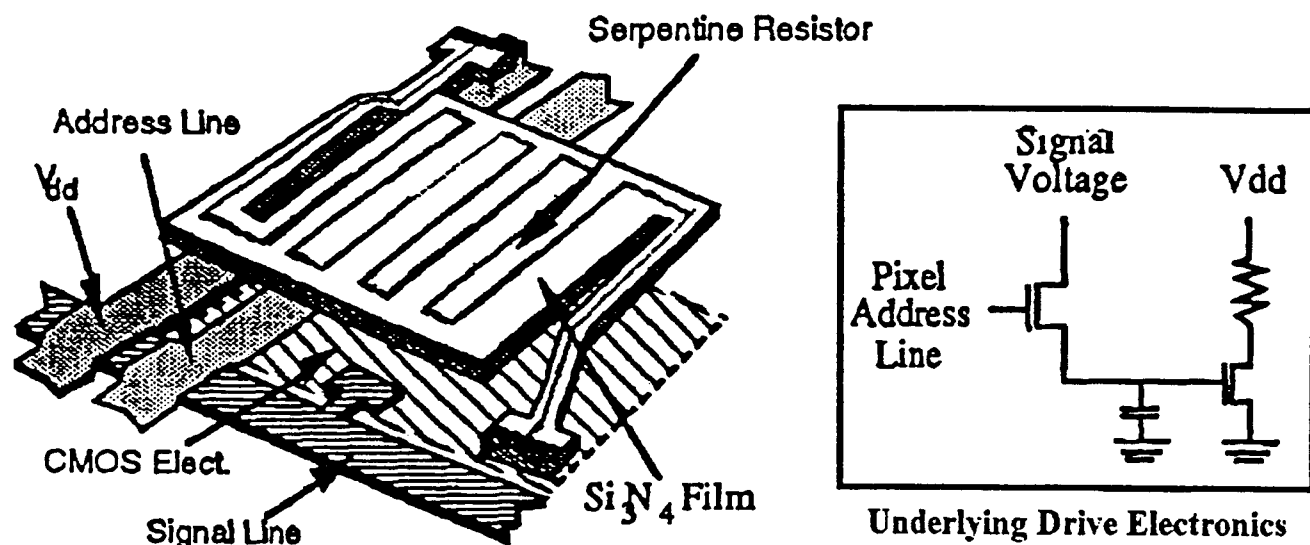


Figure 3. Honeywell Suspended Membrane Resistor Example

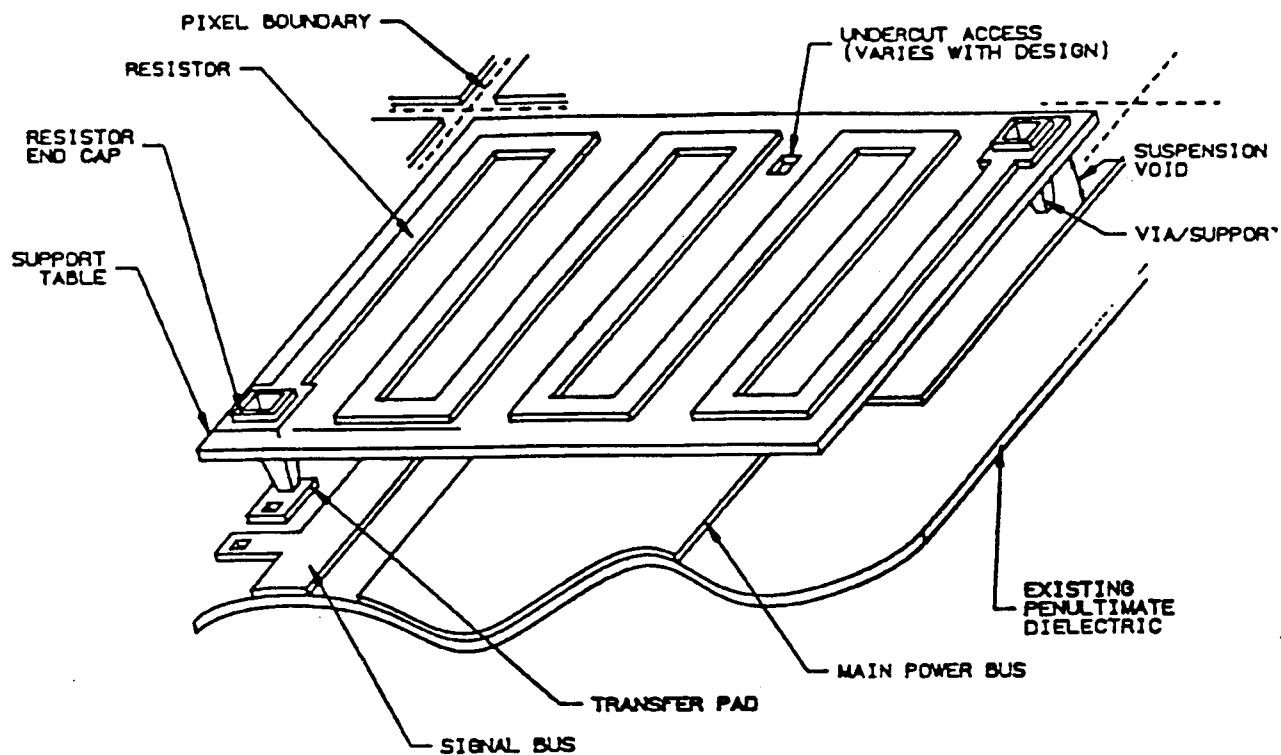


Figure 4. British Aerospace Suspended Membrane Resistor

### III. AUSTRALIAN RESISTOR ARRAY PHYSICAL CHARACTERISTICS

The Australian resistor array is a specialized case of the general thin-film approach. Although the physics of operation is the same as that for the larger arrays, the tested device has several favorable differences. First, yield is not a problem because the array is much smaller with far fewer elements. Second, fill factor is significantly better at approximately 80 percent. Third, the uniformity is much better across the smaller array as would be expected. Finally, the speed of response is significantly better than that associated with the larger arrays. Figure 5 provides a cross sectional view of the Australian resistor. The resistor is made by placing an insulated layer (polyimide) on a substrate (silicon) and then etching the resistor element (nichrome) on the insulating layer. In order to isolate the individual elements and, accordingly, limit cross-talk, gaps are etched into the insulating layer between the elements. Also, because heating of the substrate will occur, the substrate is placed on a thermally large heat sink which can be cooled to 77 K if below ambient radiances are required. Testing was done at both room temperature (ambient) and inside a dewar at a cryogenic (liquid nitrogen) temperature to accurately characterize performance. Figure 5 provides a magnified view of the resistor array tested. According to the test data delivered with the chips (Appendix B), a resistance of approximately 120 ohms was quoted. The maximum drive power recommended was 1.1 watts which correlates to a maximum drive current of approximately 90 mA at a maximum drive voltage of 11.2 volts. The resistor elements physical dimensions are 240 micron x 400 micron.

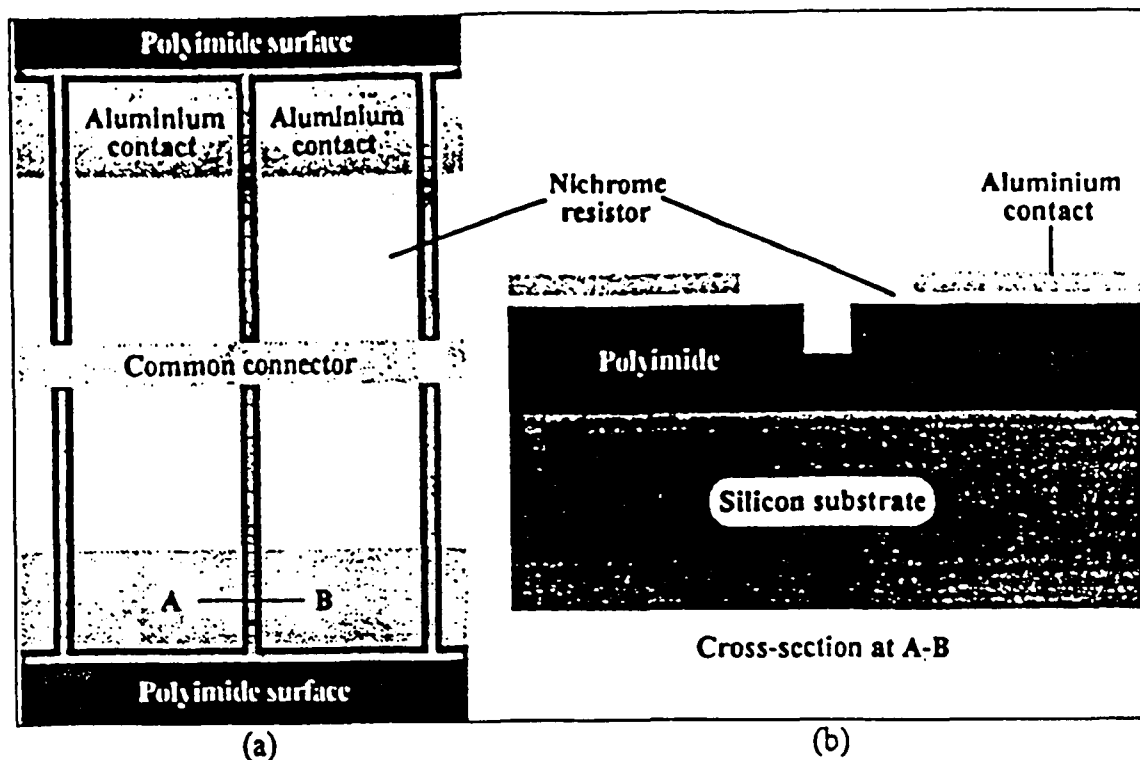


Figure 5. Australian Resistor

#### IV. MEASUREMENT METHODS

Several different optical setups were used to collect the various pieces of data necessary to fully characterize the array. Figure 6 shows the test setup used to determine the output versus power (current x voltage) characteristics of the devices. In addition to the dewar/array assembly, the key components used in the test are the IR cameras (MWIR or LWIR), image processing computer, the intermediate focusing lens, the external power supply, the interface buffer box, and the two digital multimeters. In this setup a known voltage and current were applied to discrete resistor elements. These were recorded into a table of raw data along with the resultant IR radiometer measurement of the effective temperature. For calibration purposes, a black body was placed in the position of the dewar/array assembly and the data taken again. These measurements were taken for several individual elements in both bands to obtain a representative curve showing the output versus power characteristic of the array. Examples of this data for the resistors identified in the legend are shown in Figures 7 and 8 for the cooled and uncooled substrate in the 3 to 5 micron band and in Figures 9 and 10 for the cooled and uncooled substrate in the 8 to 12 micron band. In addition to these tests, measurements were taken to characterize the temporal response of the individual elements. The optical test setup shown in Figure 11 was used to accomplish this task. In addition to the dewar/array assembly, the key components used in the test are the calibrated IR detector (MWIR only), the pulse generator, the buffer interface box, the digital oscilloscope, and the pen plotter. These measurements were taken for several individual elements to obtain a representative curve showing the rise and fall times for a step input. An example of the data is shown in Figure 12. Appendix A provides a complete listing of the collected data in both graphical and tabular form. In addition, Appendix A provides a brief discussion of the calibration procedure applied to radiometric measurements.

## V. SUMMARY

Analysis of the test data indicates that the resistor arrays performed well enough to merit further consideration for possible application in the United States. The devices demonstrated a reasonable dynamic range and could achieve a high frame rate. The only problem which was evident in the testing involved the cryogenic cooling of the substrate to 77 K. Based on the tests performed under this condition it was clear that some sort of thermal expansion mismatch existed in the multilayer architecture of the resistor elements and drive network. During the referenced tests, a high percentage of the elements became inactive following the cooling process. This is documented in Appendix A. The tested device was returned for examination by the manufacturer who verified the initial impression based on the data collected. However, in the uncooled state, the device performed well enough to meet performance requirements. Accordingly, if ambient temperatures are all that is required the device will perform adequately in that application. Still the manufacturer is correcting the problem and will provide replacements at no cost which should work in a cooled dewar environment.

In conclusion, it is apparent that it has limitations which will prohibit its wide application in HWIL simulators within the United States. However, given that there is no ideal IR projector which has the frame rate, dynamic range, temperature resolution, spatial resolution, flicker, and physical size characteristics required to cover all HWIL simulation requirements, several specific simulations can be carried out with the individual devices currently available. An IR projection system based on this approach appears to have greatest potential for future support of complete end to end HWIL simulations of IR guided weapon systems which utilize linear arrays of detectors and in which true thermal IR radiation is a requirement. In most cases photon integration is adequate and the current generation of IR laser diodes which are based on edge emitting technologies will out perform the small arrays in this scenario. Still, this technique could provide a small, inexpensive, dynamic source which at least solve some of the problems which have traditionally faced the Government R&D laboratories involved in HWIL simulations of IR guided systems.

In order to further evaluate the devices for application in the United States, two of the remaining three devices were provided to the U. S. Navy (Naval Air Warfare Center) and Eglin Air Force Base for additional testing. As this test data becomes available it will be distributed to the personnel shown in the distribution list of this report.

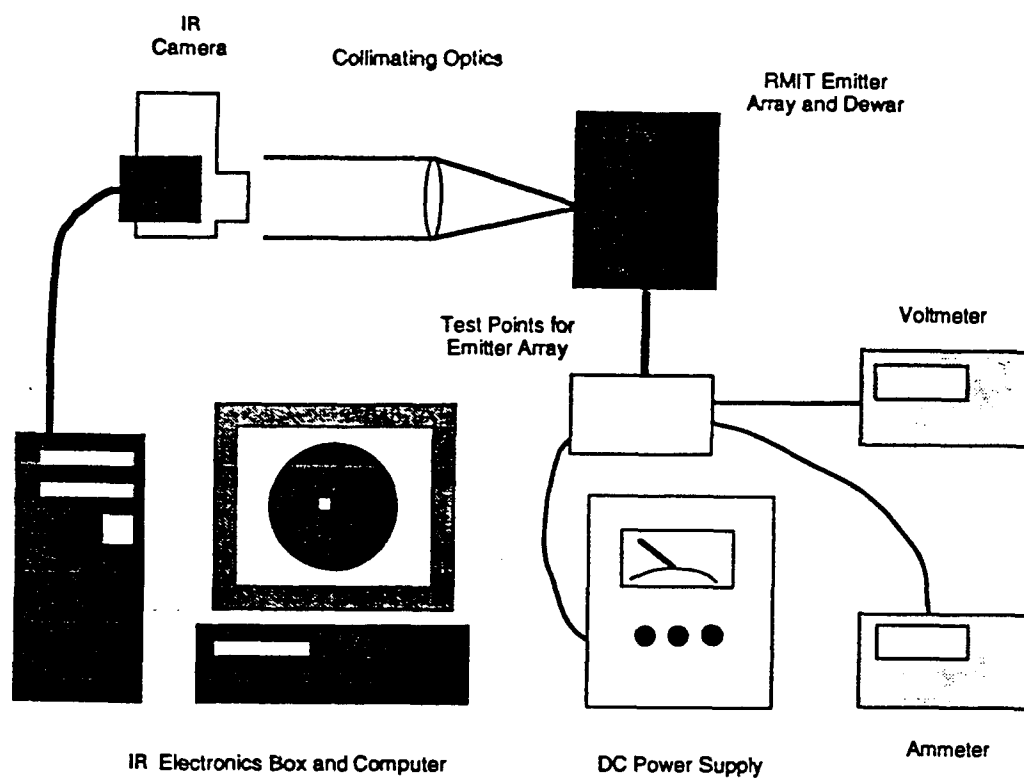


*Figure 6. Output Versus Power Test Setup*

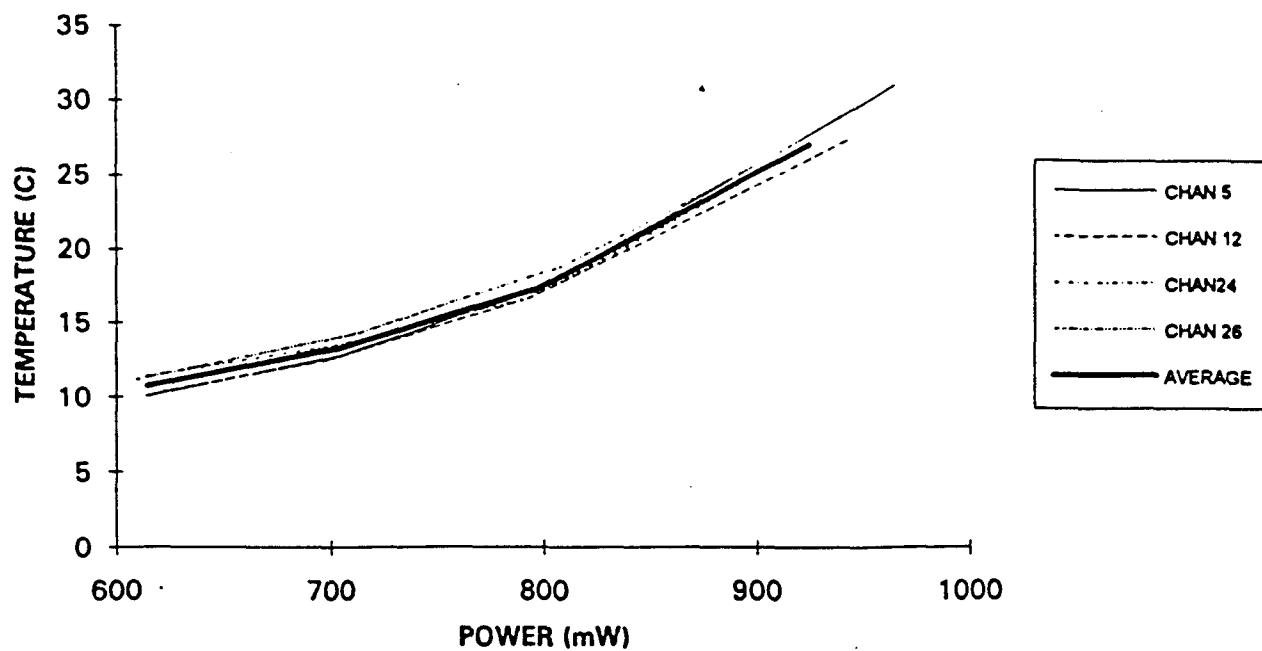


*Figure 7. 3 to 5 Microns, Substrate at 77 K*

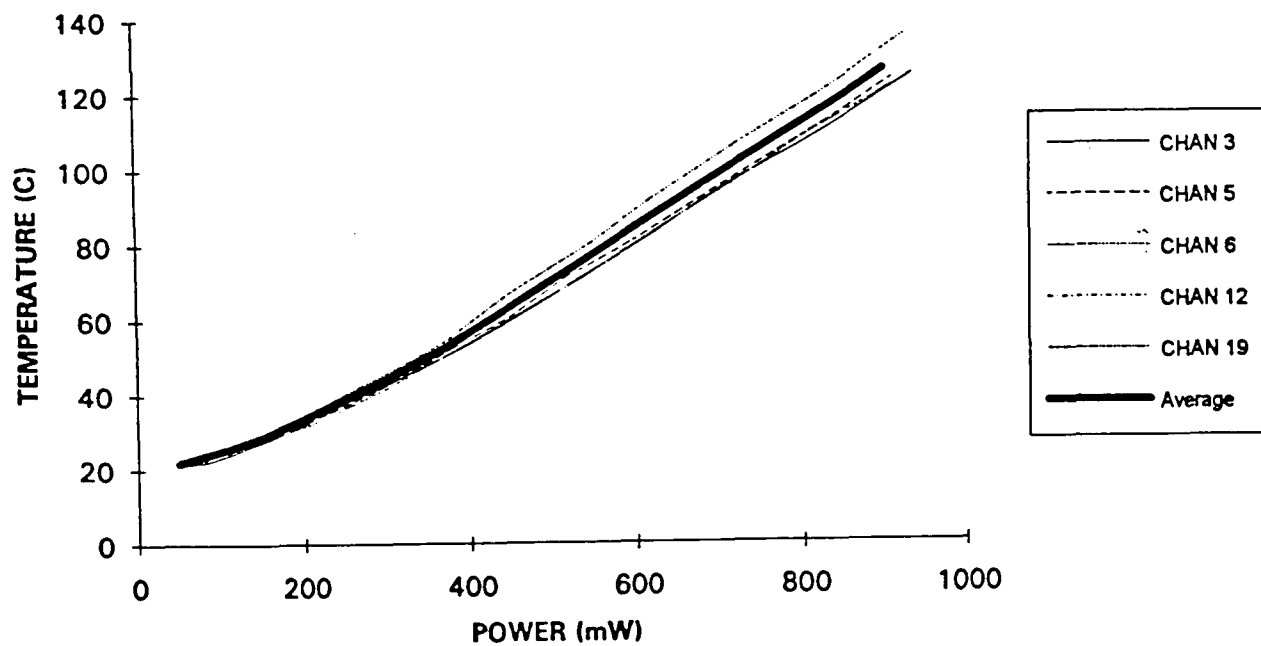


Figure 8. 3 to 5 Microns, Substrate at Ambient Temperature

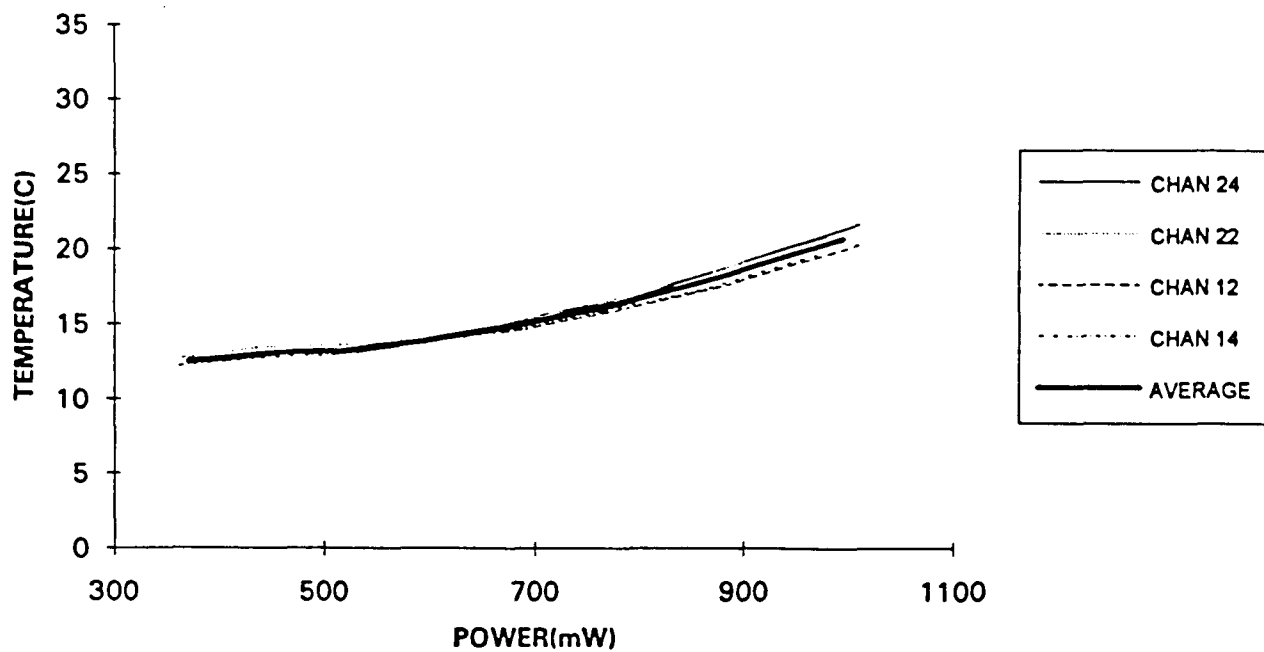


Figure 9. 8 to 12 Microns, Substrate at 77 K

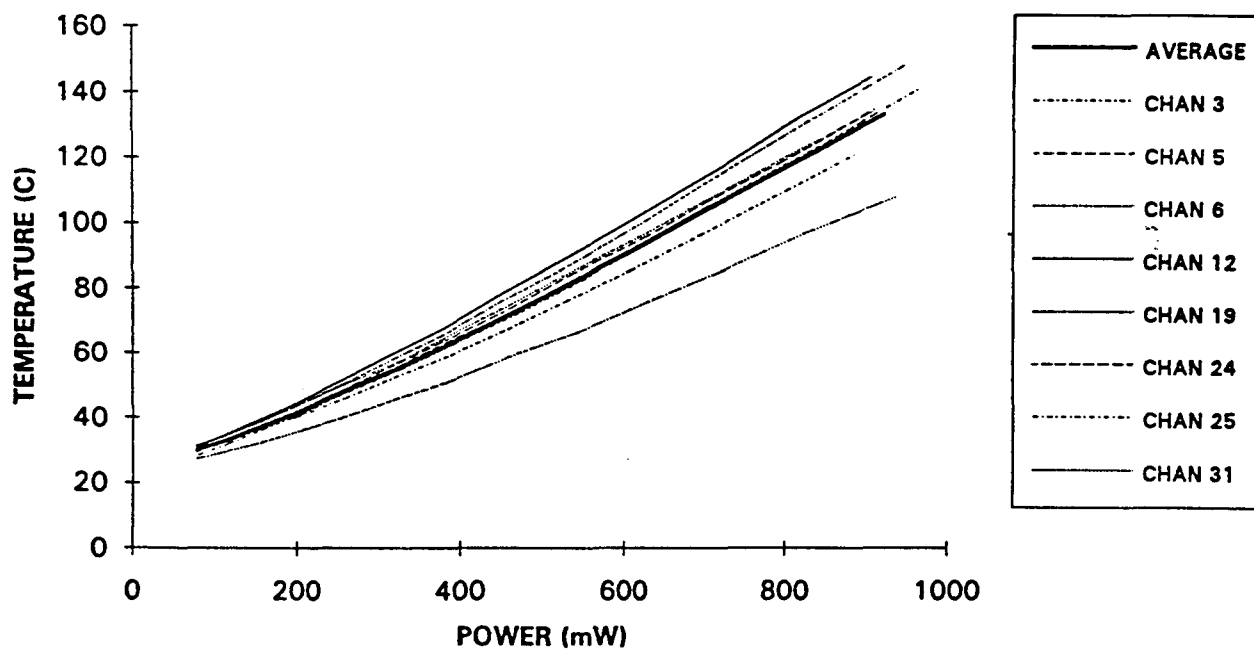


Figure 10. 8 to 12 Microns, Substrate at Ambient Temperature

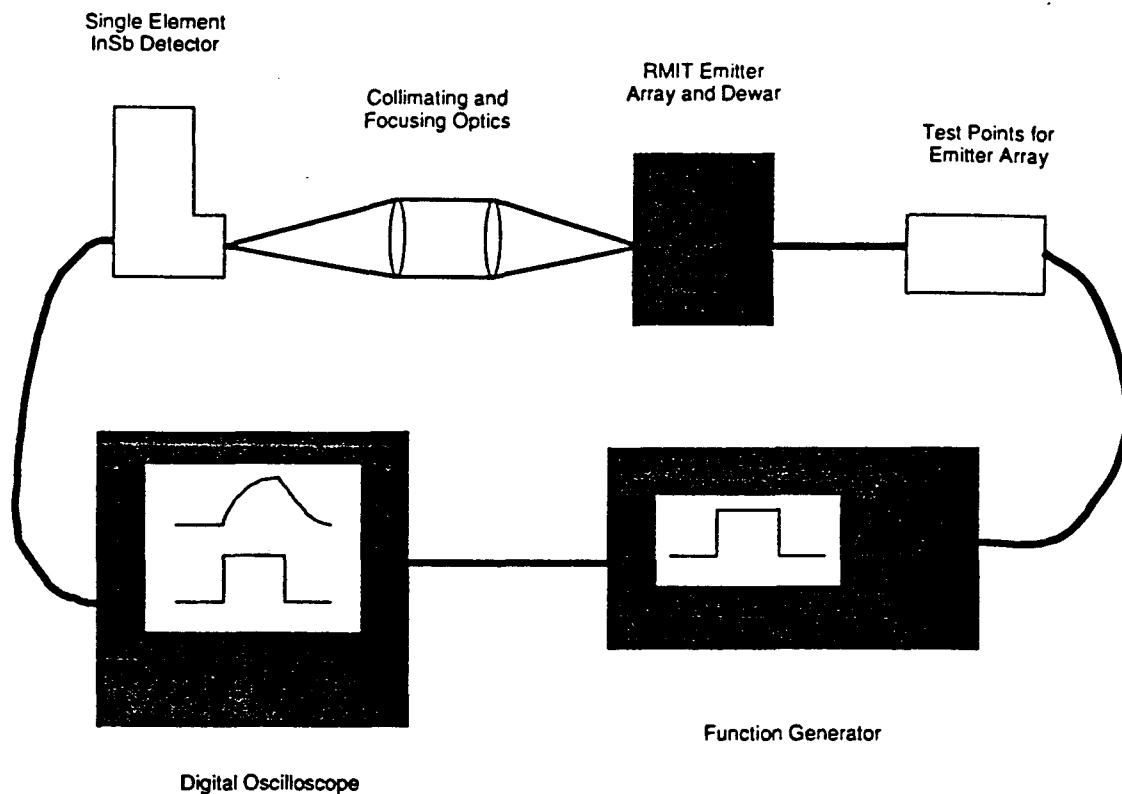


Figure 11. Temporal Response Test Setup

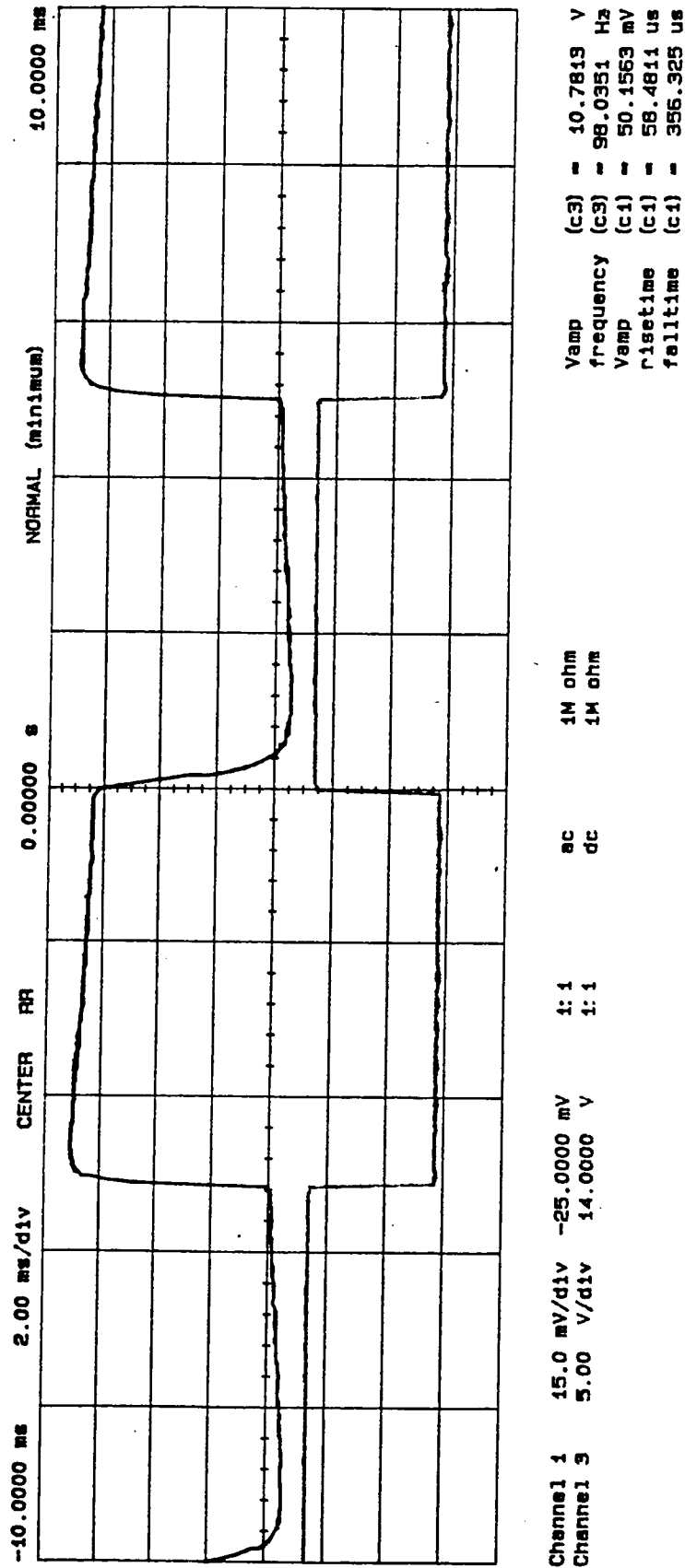


Figure 12. Example Curve of Rise and Fall Time for a Step Input

## REFERENCES

1. A. P. Pritchard, M. C. Hebborn, S. P. Lake, I. M. Sturland, "A High Fill Factor Suspended Resistor IR Scene Generator: Design, Fabrication, and Preliminary Performance," Characterization, Propagation, and Simulation of Sources and Backgrounds III, SPIE Proceedings, Vol. 1967, pp. 15-26, 12-13 April 1993.
2. O. M. Williams, G. K. Reeves, "Thermal Comparison of Emissive Infrared Projector Devices," Characterization, Propagation, and Simulation of Sources and Backgrounds III, SPIE Proceedings, Vol. 1967, pp. 2-14, 12-13 April 1993.
3. B. E. Cole, et. al., "Ultralow-Power Scene Projector for Targets Against Space Backgrounds," Characterization, Propagation, and Simulation of Sources and Backgrounds III, SPIE Proceedings, Vol. 1967, pp. 39-50, 12-13 April 1993.
4. O. M. Williams, "Infrared Projector Effective Blackbody Temperature," Optical Engineering, Vol. 33, No. 1, pp. 230-236, January 1994.
5. O. M. Williams, "Infrared Projector Optical Design Considerations," Optical Engineering, Vol. 33, No. 1, pp. 237-241, January 1994.
6. S. B. Mobley, J. A. Buford, "Hardware-In-The-Loop Infrared Projector Technology," Characterization, Propagation, and Simulation of Sources and Backgrounds II, SPIE Proceedings, Vol. 1687, pp. 14-21, April 1992.

**APPENDIX A**  
**TEST DATA**

**APPENDIX A  
TEST DATA**

**TABLE OF CONTENTS**

	<u>Page</u>
A.I. MWIR TEMPERATURE VERSES POWER DATA – UNCOOLED SUBSTRATE .....	A-2
A.II. MWIR TEMPERATURE VERSES POWER DATA – COOLED SUBSTRATE .....	A-7
A.III. LWIR TEMPERATURE VERSES POWER DATA – UNCOOLED SUBSTRATE .....	A-10
A.IV. LWIR TEMPERATURE VERSUS POWER DATA – COOLED SUBSTRATE .....	A-17
A.V. TEMPORAL RESPONSE DATA .....	A-21
A.VI. CALIBRATION PROCEDURE .....	A-25

## A.I. MWIR TEMPERATURE VERSES POWER DATA – UNCOOLED SUBSTRATE

The tables contained in this section provide the measured values for current, voltage, and temperature (in celsius) of channels (i.e. resistor elements) 3, 5, 6, 12, 19, 24, and 25. This data is shown in columns 1, 2, and 3, respectively. From these measurements, values for power, calibrated temperature, and resistance were calculated. These calculated values are presented in columns 4, 5, and 6. A curve is shown at the end of Section A.I showing the cumulative voltage verses current characteristics of all the measured elements identified above.

### 3 TO 5 MICRONS, SUBSTRATE AT AMBIENT TEMPERATURE

CHAN 3					
I(mA)	Volts(V)	POWER	T(meas)	T(cal)	R (ohms)
20.95	2.62	54.889	24.8	21.5696	125.0597
25.2	3.16	79.632	25.5	22.2955	125.3968
30	3.75	112.5	27.8	24.6806	125
36.2	4.52	163.624	31.8	28.8286	124.8619
40.1	5.01	200.901	35.1	32.2507	124.9377
45	5.63	253.35	40.9	38.2653	125.1111
50.26	6.28	315.6328	46.8	44.3836	124.9503
55.1	6.88	379.088	53.3	51.1241	124.8639
60.4	7.55	456.02	62.1	60.2497	125
64.4	8.05	518.42	70.1	68.5457	125
70.3	8.77	616.531	82.7	81.6119	124.7511
75.6	9.44	713.664	96	95.404	124.8677
79.99	9.98	798.3002	106	105.774	124.7656
86.7	10.81	937.227	124	124.44	124.6828
		AVERAGE RESISTANCE ->			124.9463

CHAN 5					
I(mA)	Volts(V)	POWER	T(meas)	T(cal)	R (ohms)
20.3	2.55	51.765	25	21.777	125.6158
25	3.14	78.5	26	22.814	125.6
30.2	3.8	114.76	29	25.925	125.8278
35.5	4.4	156.2	32.3	29.3471	123.9437
40.6	5.1	207.06	36	33.184	125.6158
45	5.6	252	40.2	37.5394	124.4444
50.7	6.35	321.945	47.4	45.0058	125.2465
55.4	6.9	382.26	54.8	52.6796	124.5487
60.1	7.5	450.75	62.5	60.6645	124.792
64.1	8.1	519.21	72.6	71.1382	126.3651
69.1	8.65	597.715	81.6	80.4712	125.1809
75.3	9.4	707.82	96	95.404	124.834
80	10	800	108	107.848	125
85.3	10.7	912.71	123	123.403	125.4396
88.2	11.05	974.61	130	130.662	125.2834
		AVERAGE RESISTANCE ->			125.1825

### 3 TO 5 MICRONS, SUBSTRATE AT AMBIENT TEMPERATURE

CHAN 6					
I(mA)	Volts(V)	POWER	T(meas)	T(cal)	R (ohms)
19.6	2.5	49	25	21.777	127.551
24.8	3.1	76.88	27	23.851	125
29.5	3.7	109.15	29	25.925	125.4237
35.1	4.4	154.44	31.5	28.5175	125.3561
40.3	5.1	205.53	35	32.147	126.5509
45	5.7	256.5	40	37.332	126.6667
50.7	6.4	324.48	47	44.591	126.2327
55.9	7	391.3	55	52.887	125.2236
60.5	7.6	459.8	63	61.183	125.6198
65.3	8.2	535.46	72	70.516	125.5743
70.4	8.85	623.04	84	82.96	125.7102
75.6	9.5	718.2	96	95.404	125.6614
80.8	10.1	816.08	110	109.922	125
85.2	10.7	911.64	121	121.329	125.5869
88.1	11	969.1	129	129.625	124.8581
		AVERAGE RESISTANCE ->			125.7344

CHAN 12					
I(mA)	Volts(V)	POWER	T(meas)	T(cal)	R (ohms)
20.4	2.56	52.224	25.6	22.3992	125.4902
24.9	3.1	77.19	27.3	24.1621	124.498
30.1	3.8	114.38	29.8	26.7546	126.2458
34.9	4.4	153.56	32.4	29.4508	126.0745
40.3	5.07	204.321	37.6	34.8432	125.8065
45.3	5.7	258.21	42.3	39.7171	125.8278
49.8	6.25	311.25	48.5	46.1465	125.502
55	6.9	379.5	55	52.887	125.4545
60.4	7.6	459.04	66.5	64.8125	125.8278
64.9	8.1	525.69	75	73.627	124.8074
70.2	8.8	617.76	88.4	87.5228	125.3561
75	9.4	705	99.4	98.9298	125.3333
80.3	10.1	811.03	112.5	112.5145	125.7783
84.6	10.6	896.76	125	125.477	125.2955
88.38	11.1	981.018	134	134.81	125.594
		AVERAGE RESISTANCE ->			125.5261

# 3 TO 5 MICRONS, SUBSTRATE AT AMBIENT TEMPERATURE

CHAN 19					
I(mA)	Volts(V)	POWER	T(meas)	T(cal)	R (ohms)
21.6	2.74	59.184	26.2	23.0214	126.8519
24.8	3.15	78.12	28.2	25.0954	127.0161
30.1	3.81	114.681	30.1	27.0657	126.5781
35.1	4.45	156.195	33	30.073	126.7806
40.3	5.1	205.53	38	35.258	126.5509
45.9	5.82	267.138	45	42.517	126.7974
50.6	6.41	324.346	50.7	48.4279	126.6798
54.4	6.89	374.816	57	54.961	126.6544
58.9	7.47	439.983	67	65.331	126.8251
65.7	8.32	546.624	81	79.849	126.6362
70	8.84	618.8	92	91.256	126.2857
75.5	9.55	721.025	106	105.774	126.4901
80.3	10.15	815.045	118	118.218	126.401
85.6	10.83	927.048	134	134.81	126.5187
87.5	11	962.5	138	138.958	125.7143
		AVERAGE RESISTANCE ->			126.5854

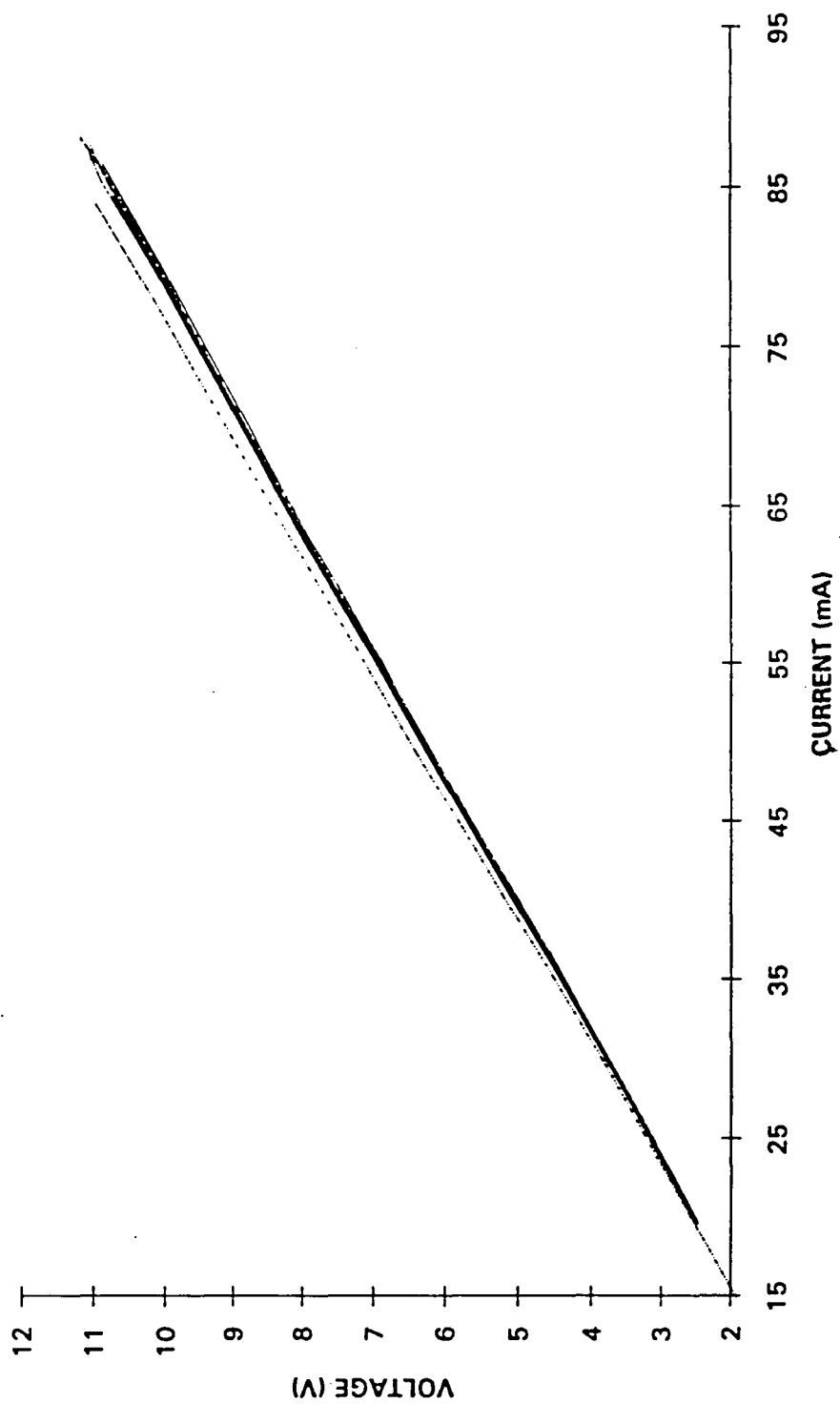
CHAN 24					
I(mA)	Volts(V)	POWER	T(meas)	T(cal)	R (ohms)
19.7	2.5	49.25	26	22.814	126.9036
24.9	3.1	77.19	28	24.888	124.498
29.6	3.7	109.52	30	26.962	125
34.8	4.4	153.12	33	30.073	126.4368
40.1	5	200.5	38	35.258	124.6883
45.1	5.66	255.266	44.2	41.6874	125.4989
50.8	6.4	325.12	51.6	49.3612	125.9843
55	6.9	379.5	59	57.035	125.4545
60.2	7.6	457.52	69	67.405	126.2458
64.8	8.1	524.88	78	76.738	125
70.6	8.86	625.516	93	92.293	125.4958
74.9	9.4	704.06	104	103.7	125.5007
80.6	10.1	814.06	119	119.255	125.3102
84.9	10.6	899.94	131	131.699	124.8528
88.3	11.1	980.13	140	141.032	125.7078
		AVERAGE RESISTANCE ->			125.5052

### 3 TO 5 MICRONS, SUBSTRATE AT AMBIENT TEMPERATURE

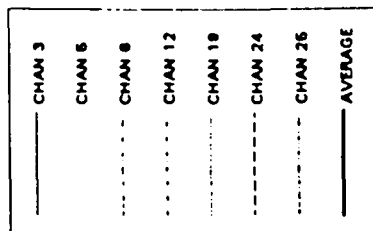
CHAN 25					
I(mA)	Volts(V)	POWER	T(meas)	T(cal)	R (ohms)
14.9	1.92	28.608	25.4	22.1918	128.8591
20.07	2.59	51.9813	26.7	23.5399	129.0483
25.19	3.25	81.8675	27.6	24.4732	129.0195
29.9	3.85	115.115	30.4	27.3768	128.7625
35.05	4.52	158.426	34	31.11	128.9586
40.2	5.19	208.638	38.5	35.7765	129.1045
44.87	5.79	259.7973	43.5	40.9615	129.0394
49.4	6.4	316.16	49.7	47.3909	129.5547
55.9	7.23	404.157	60.5	58.5905	129.3381
60.97	7.88	480.4436	70.4	68.8568	129.2439
65.97	8.54	563.3838	81	79.849	129.4528
69.4	8.99	623.906	89	88.145	129.5389
75.8	9.82	744.356	106	105.774	129.5515
79.7	10.33	823.301	117	117.181	129.611
84.2	10.9	917.78	128	128.588	129.4537
87.7	11.322	992.9394	138	138.958	129.0992
		AVERAGE RESISTANCE ->			129.2272

### AVERAGE OF CHANNELS 3, 5, 6, 12, 19, 24, AND 25

I(mA)	Volts(V)	POWER	T(meas)	T(cal)	R (ohms)
19.63571	2.484286	49.27429	25.42857	22.22143	126.5187
24.23857	3.048571	74.21333	26.95714	23.80656	125.7736
29.24143	3.687143	108.1226	29.04286	25.96944	126.0931
34.5	4.345714	150.322	32.05714	29.09526	125.9627
39.53571	4.985714	197.4669	36.24286	33.43584	126.1066
44.5	5.614286	250.1574	41.58571	38.97639	126.1637
49.67571	6.268571	311.7959	47.92857	45.55393	126.1899
54.31429	6.838571	371.8034	54.82857	52.70923	125.9074
59.48571	7.507143	446.7529	64.37143	62.60517	126.2008
64.31	8.107143	521.5325	74.15714	72.75296	126.0635
69.51	8.758571	608.9637	86.1	85.1377	126.0045
74.47143	9.382857	699.0964	98.05714	97.53726	125.9927
79.68429	10.03571	799.8387	111.3571	111.3294	125.9435
84.57143	10.65286	901.2323	125	125.477	125.9628



3 to 5 Microns, Substrate at Ambient Temperature



## **A.II. MWIR TEMPERATURE VERSES POWER DATA – COOLED SUBSTRATE**

The tables contained in this section provide the measured values for current, voltage, and temperature (in celsius) of channels (i.e. resistor elements) 5, 12, 24, and 26. This data is shown in columns 1, 2, and 3, respectively. From these measurements, values for power, calibrated temperature, and resistance were calculated. These calculated values are presented in columns 4, 5, and 6. A curve is shown at the end of Section A.II showing the cumulative voltage verses current characteristics of all the measured elements identified above.

### 3 TO 5 MICRONS, SUBSTRATE AT 77 K

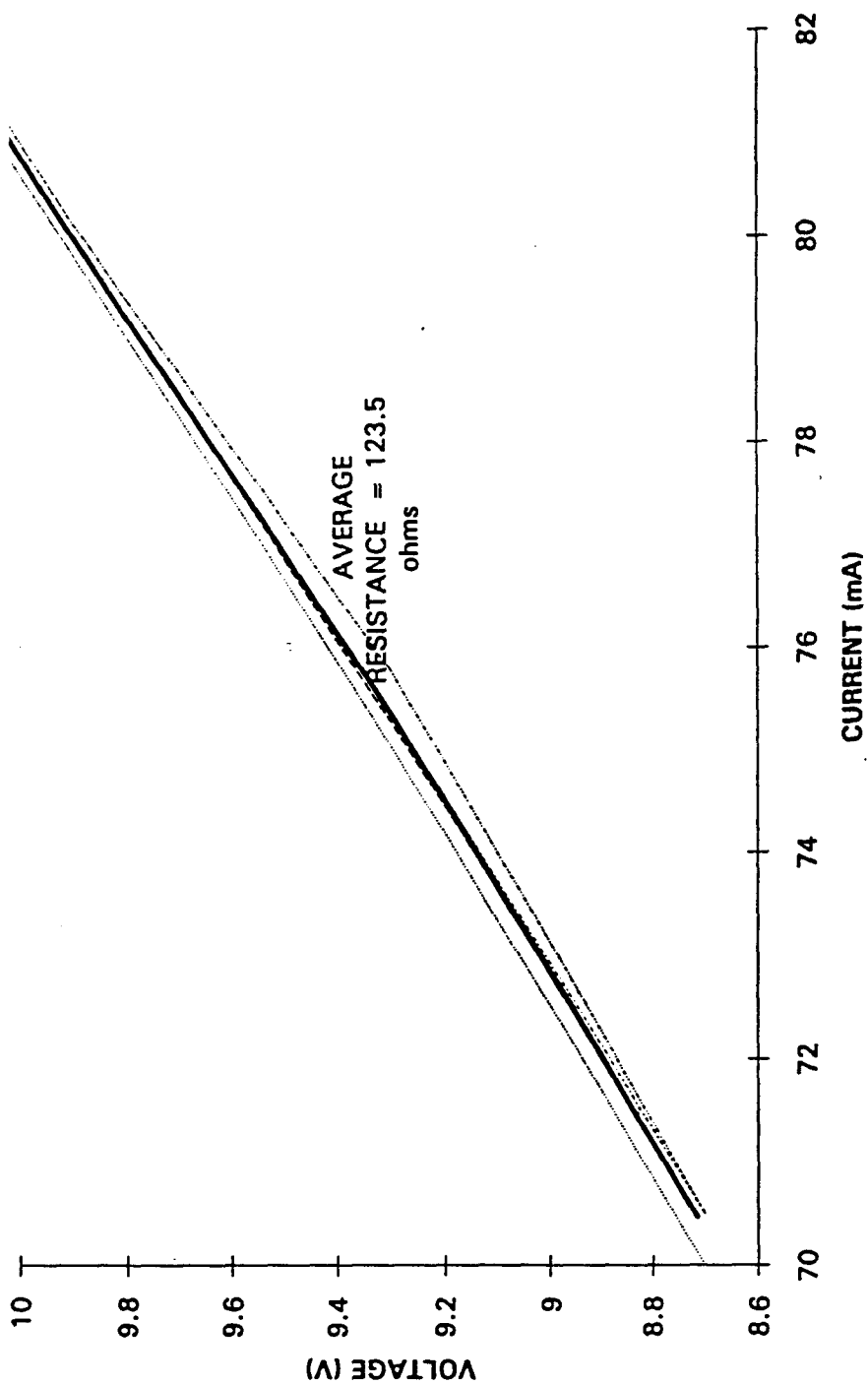
CHAN 5					
I(mA)	V(v)	P(mW)	T(meas)	T(cal)	R (ohms)
70.5	8.7	613.35	13.7	10.0589	123.4043
75.8	9.3	704.94	16.3	12.7551	122.6913
80.2	9.9	793.98	20.4	17.0068	123.4414
88.5	10.9	964.65	33.8	30.9026	123.1638
					123.1752

CHAN 12					
I(mA)	V(v)	P(mW)	T(meas)	T(cal)	R (ohms)
70.9	8.76	621.084	14	10.37	123.5543
75.3	9.3	700.29	16.1	12.5477	123.506
80.1	9.9	792.99	20	16.592	123.5955
87.5	10.8	945	30.5	27.4805	123.4286
					123.5211

CHAN 24					
I(mA)	V(v)	P(mW)	T(meas)	T(cal)	R (ohms)
70.5	8.7	613.35	15	11.407	123.4043
75.4	9.3	701.22	17	13.481	123.3422
80.1	9.9	792.99	20	16.592	123.5955
85.1	10.5	893.55	27.4	24.2658	123.3843
89	10.97	976.33	35.4	32.5618	123.2584
					123.3969

CHAN 26					
I(mA)	V(v)	P(mW)	T(meas)	T(cal)	R (ohms)
70	8.7	609	14.8	11.1996	124.2857
75.9	9.4	713.46	17.8	14.3106	123.8472
80.7	10	807	22	18.666	123.9157
85	10.5	892.5	28.1	24.9917	123.5294
88.1	10.9	960.29	33.2	30.2804	123.723
					123.8602

AVERAGE OF CHANNELS 5, 12, 24, & 26					
I(mA)	V(v)	P(mW)	T(meas)	T(cal)	R (ohms)
70.475	8.715	614.196	14.375	10.75888	123.6609
75.6	9.325	704.9775	16.8	13.2736	123.3466
80.275	9.925	796.74	20.6	17.2142	123.6375
86.525	10.675	923.925	29.95	26.91015	123.3747
					123.5049



### **A.III. LWIR TEMPERATURE VERSES POWER DATA – UNCOOLED SUBSTRATE**

The tables contained in this section provide the measured values for current, voltage, and temperature (in celsius) of channels (i.e. resistor elements) 3, 5, 6, 12, 19, 24, 25, and 31. This data is shown in columns 1, 2, and 3, respectively. From these measurements, values for power, calibrated temperature, and resistance were calculated. These calculated values are presented in columns 4, 5, and 6. A curve is shown at the end of Section A.III showing the cumulative voltage verses current characteristics of all the measured elements identified above.

# 8 TO 12 MICRONS, SUBSTRATE AT AMBIENT TEMPERATURE

CHAN 3					
I(mA)	V(v)	P(mW)	T(meas)	T(cal)	R (ohms)
25.7	3.2	82.24	26.6	30.0924	124.51
30.4	3.8	115.52	28.1	32.6634	125.00
34.77	4.3	149.511	30.1	36.0914	123.67
40.06	5	200.3	32.6	40.3764	124.81
45.7	5.7	260.49	35.8	45.8612	124.73
50.7	6.3	319.41	39.4	52.0316	124.26
55.8	6.96	388.368	43.5	59.059	124.73
60.5	7.55	456.775	48.1	66.9434	124.79
65.3	8.1	528.93	53.1	75.5134	124.04
70.1	8.7	609.87	58.6	84.9404	124.11
74.9	9.3	696.57	64.8	95.5672	124.17
80.2	9.99	801.198	72.8	109.2792	124.56
84.5	10.5	887.25	79.4	120.5916	124.26
87.9	10.93	960.747	84.3	128.9902	124.35
		AVERAGE RESISTANCE ->			124.4282

CHAN 5					
I(mA)	V(v)	P(mW)	T(meas)	T(cal)	R (ohms)
25	3.14	78.5	26.6	30.0924	125.6
29.8	3.74	111.452	28.4	33.1776	125.5034
35.48	4.45	157.886	31	37.634	125.4228
40.7	5.1	207.57	34	42.776	125.3071
44.9	5.63	252.787	36.6	47.2324	125.3898
50	6.27	313.5	40.6	54.0884	125.4
54.4	6.8	369.92	44.8	61.2872	125
60.1	7.53	452.553	50.3	70.7142	125.2912
65.8	8.24	542.192	57.3	82.7122	125.228
70.1	8.78	615.478	62.8	92.1392	125.2496
75.3	9.43	710.079	70.4	105.1656	125.2324
79.6	9.96	792.816	76.4	115.4496	125.1256
85.3	10.7	912.71	86.5	132.761	125.4396
88.4	11.05	976.82	90	138.76	125
		AVERAGE RESISTANCE ->			125.2992

8 TO 12 MICRONS, SUBSTRATE AT AMBIENT TEMPERATURE

CHAN 6					
I(mA)	V(v)	P(mW)	T(meas)	T(cal)	R (ohms)
24.9	3.14	78.186	27.4	31.4636	126.1044
29.7	3.7	109.89	29	34.206	124.5791
35.4	4.45	157.53	31.7	38.8338	125.7062
40.1	5	200.5	34.5	43.633	124.6883
44.76	5.6	250.656	37.7	49.1178	125.1117
50.5	6.4	323.2	42.2	56.8308	126.7327
55.1	6.9	380.19	46.6	64.3724	125.2269
60.8	7.6	462.08	52.6	74.6564	125
64.8	8.1	524.88	57.6	83.2264	125
70.7	8.9	629.23	65.3	96.4242	125.884
75.4	9.5	716.3	72.1	108.0794	125.9947
80.7	10.1	815.07	80	121.62	125.1549
85	10.7	909.5	87	133.618	125.8824
88.8	11.14	989.232	93.6	144.9304	125.4505
		AVERAGE RESISTANCE ->			125.4654

CHAN 12					
I(mA)	V(v)	P(mW)	T(meas)	T(cal)	R (ohms)
25	3.1	77.5	27.2	31.1208	124
29.4	3.7	108.78	29.1	34.3774	125.8503
35.3	4.4	155.32	32.1	39.5194	124.6459
39.6	5	198	34.9	44.3186	126.2626
44.8	5.64	252.672	38.8	51.0032	125.8929
50.5	6.35	320.675	43.9	59.7446	125.7426
54.7	6.9	377.43	48.1	66.9434	126.1426
60	7.5	450	54.5	77.913	125
64.7	8.1	524.07	60.3	87.8542	125.1932
70.8	8.9	630.12	69.2	103.1088	125.7062
75.5	9.5	717.25	76.5	115.621	125.8278
80.9	10.1	817.09	85.9	131.7326	124.8455
85	10.67	906.95	93.1	144.0734	125.5294
88.55	11.1	982.905	99.7	155.3858	125.3529
		AVERAGE RESISTANCE ->			125.428

# 8 TO 12 MICRONS, SUBSTRATE AT AMBIENT TEMPERATURE

CHAN 19					
I(mA)	V(v)	P(mW)	T(meas)	T(cal)	R (ohms)
25.36	3.2	81.152	27.3	31.2922	126.183
29.6	3.74	110.704	29.1	34.3774	126.3514
35	4.4	154	31.7	38.8338	125.7143
39.96	5.04	201.3984	34.6	43.8044	126.1261
45.1	5.7	257.07	38.3	50.1462	126.3858
50.3	6.35	319.405	42.9	58.0306	126.2425
54.56	6.9	376.464	46.9	64.8866	126.4663
59.7	7.5	447.75	53	75.342	125.6281
64.7	8.1	524.07	58.7	85.1118	125.1932
70.6	8.9	628.34	67.5	100.195	126.0623
75.7	9.55	722.935	76	114.764	126.1559
80.95	10.2	825.69	84.9	130.0186	126.0037
86.85	10.9	946.665	95.1	147.5014	125.5037
AVERAGE RESISTANCE ->					126.0013

CHAN 24					
I(mA)	V(v)	P(mW)	T(meas)	T(cal)	R (ohms)
24.97	3.1	77.407	26.2	29.4068	124.149
29.2	3.7	108.04	28	32.492	126.7123
35.5	4.45	157.975	30.9	37.4626	125.3521
39.6	5	198	33.4	41.7476	126.2626
45.3	5.7	258.21	37.4	48.6036	125.8278
50	6.3	315	41.4	55.4596	126
55.3	6.9	381.57	46.1	63.5154	124.774
59.8	7.5	448.5	50.9	71.7426	125.4181
65.6	8.2	537.92	58	83.912	125
70.8	8.9	630.12	64.7	95.3958	125.7062
75.1	9.4	705.94	70.9	106.0226	125.1664
79.7	10	797	78	118.192	125.4705
85.1	10.7	910.57	87.3	134.1322	125.7344
87.9	11	966.9	92	142.188	125.1422
AVERAGE RESISTANCE ->					125.4797

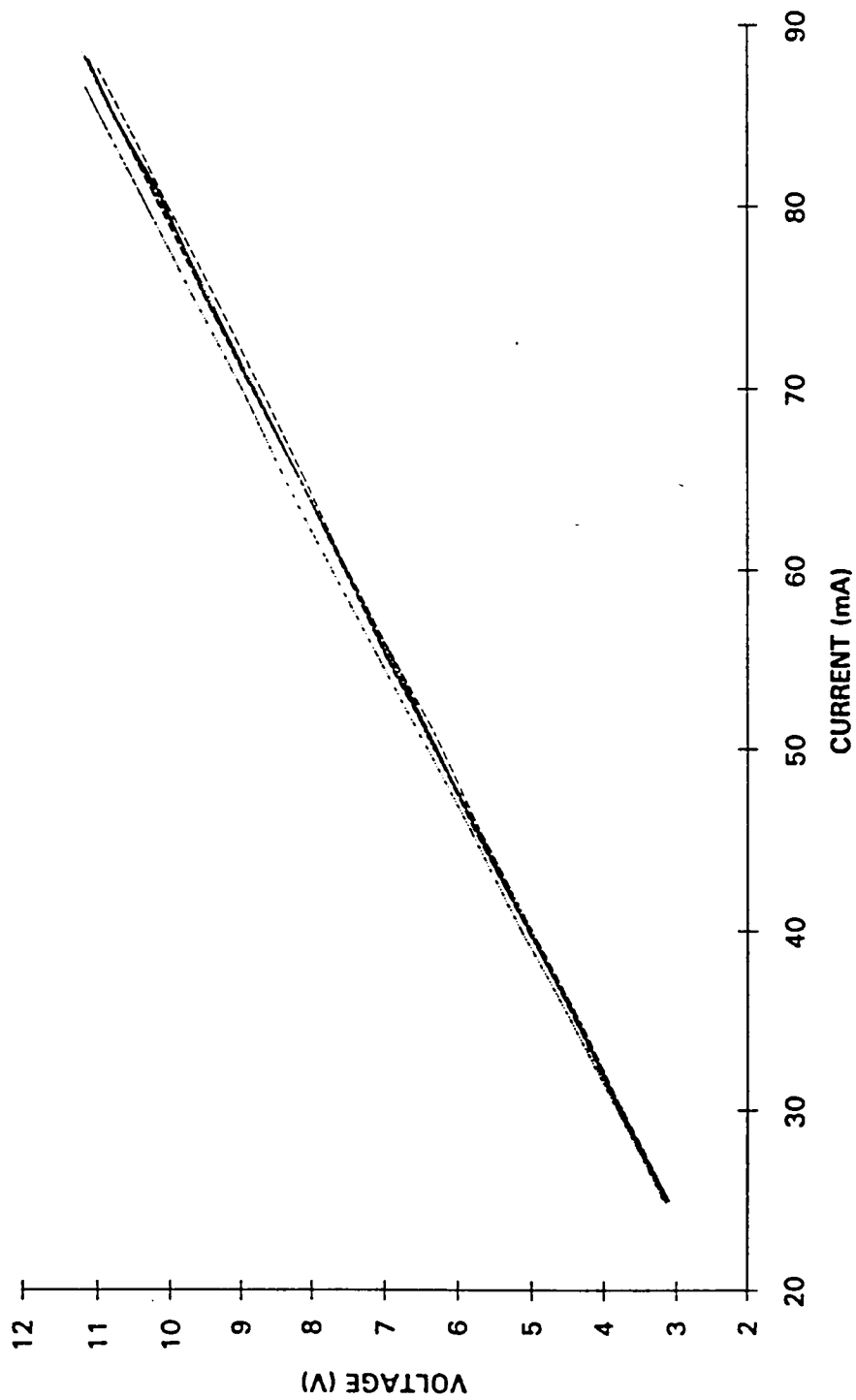
# 8 TO 12 MICRONS, SUBSTRATE AT AMBIENT TEMPERATURE

CHAN 25					
I(mA)	V(v)	P(mW)	T(meas)	T(cal)	R (ohms)
25.1	3.2	80.32	25.7	28.5498	127.49
30.3	3.86	116.958	27.7	31.9778	127.3927
35.3	4.5	158.85	30.3	36.4342	127.4788
40	5.13	205.2	33	41.062	128.25
45.5	5.8	263.9	36.9	47.7466	127.4725
50.6	6.5	328.9	40.9	54.6026	128.4585
55.3	7.1	392.63	45.4	62.3156	128.3906
60.8	7.8	474.24	51.1	72.0854	128.2895
65.4	8.4	549.36	56.8	81.8552	128.4404
70.4	9	633.6	64.3	94.7102	127.8409
75.2	9.64	724.928	71.4	106.8796	128.1915
80.8	10.35	836.28	80.4	122.3056	128.0941
86.86	11.1	964.146	90.8	140.1312	127.7918
AVERAGE RESISTANCE ->					127.9678

CHAN 31					
I(mA)	V(v)	P(mW)	T(meas)	T(cal)	R (ohms)
24.9	3.16	78.684	25	27.35	126.9076
30.1	3.82	114.982	26.3	29.5782	126.9103
35.2	4.47	157.344	28	32.492	126.9886
40.4	5.13	207.252	30.1	36.0914	126.9802
45	5.7	256.5	32.3	39.8622	126.6667
50.2	6.4	321.28	35.5	45.347	127.49
55	7	385	38.6	50.6604	127.2727
60.9	7.7	468.93	43.7	59.4018	126.4368
65.2	8.3	541.16	47.4	65.7436	127.3006
70.8	9	637.2	53.3	75.8562	127.1186
75.5	9.59	724.045	58.5	84.769	127.0199
80.7	10.2	823.14	65.1	96.0814	126.3941
85.9	10.9	936.31	71.6	107.2224	126.8917
AVERAGE RESISTANCE ->					126.9521

8 TO 12 MICRONS, SUBSTRATE AT AMBIENT TEMPERATURE

AVERAGE OF CHANNELS 3, 5, 6, 12, 19, 24, 25, & 31					
I(mA)	V(v)	P(mW)	T(meas)	T(cal)	R (ohms)
25.11625	3.155	79.24863	26.5	29.921	125.6159
29.8125	3.7575	112.0408	28.2125	32.85623	126.0377
35.24375	4.4275	156.052	30.725	37.16265	125.6251
40.0525	5.05	202.2776	33.3875	41.72618	126.0845
45.1325	5.68375	256.5356	36.725	47.44665	125.9347
50.35	6.35875	320.1713	40.85	54.5169	126.291
55.02	6.9325	381.4465	45	61.63	125.9996
60.325	7.585	457.6035	50.525	71.09985	125.7356
65.1875	8.1925	534.0728	56.15	80.7411	125.6759
70.5375	8.885	626.7448	63.2125	92.84623	125.9614
75.325	9.48875	714.7559	70.075	104.6086	125.9708
80.44375	10.1125	813.5355	77.9375	118.0849	125.709
85.56375	10.77125	921.7626	86.35	132.5039	125.8857
		AVERAGE RESISTANCE ->			125.8867



8 to 12 Microns, Substrate at Ambient Temperature

#### **A.IV. LWIR TEMPERATURE VERSUS POWER DATA – COOLED SUBSTRATE**

The tables contained in this section provide the measured values for current, voltage, and temperature (in celsius) of channels (i.e. resistor elements) 12, 14, 22, and 24. This data is shown in columns 1, 2, and 3, respectively. From these measurements, values for power, calibrated temperature, and resistance were calculated. These calculated values are presented in columns 4, 5, and 6. A curve is shown at the end of Section A.IV showing the cumulative voltage verses current characteristics of all the measured elements identified above.

# 8 TO 12 MICRONS, SUBSTRATE AT 77 K

CHAN 12					
I(mA)	V(v)	P(mW)	T(meas)	T(cal)	R (ohms)
55.87	6.86	383.2682	16.3	12.4382	122.785
60.75	7.45	452.5875	16.6	12.9524	122.6337
65.1	7.98	519.498	16.8	13.2952	122.5806
70.25	8.6	604.15	17.2	13.9808	122.4199
75.07	9.19	689.8933	17.6	14.6664	122.4191
80.25	9.8	786.45	18.4	16.0376	122.1184
85.07	10.4	884.728	19.3	17.5802	122.2523
90.94	11.12	1011.253	20.9	20.3226	122.2784
AVERAGE RESISTANCE ->					122.4359

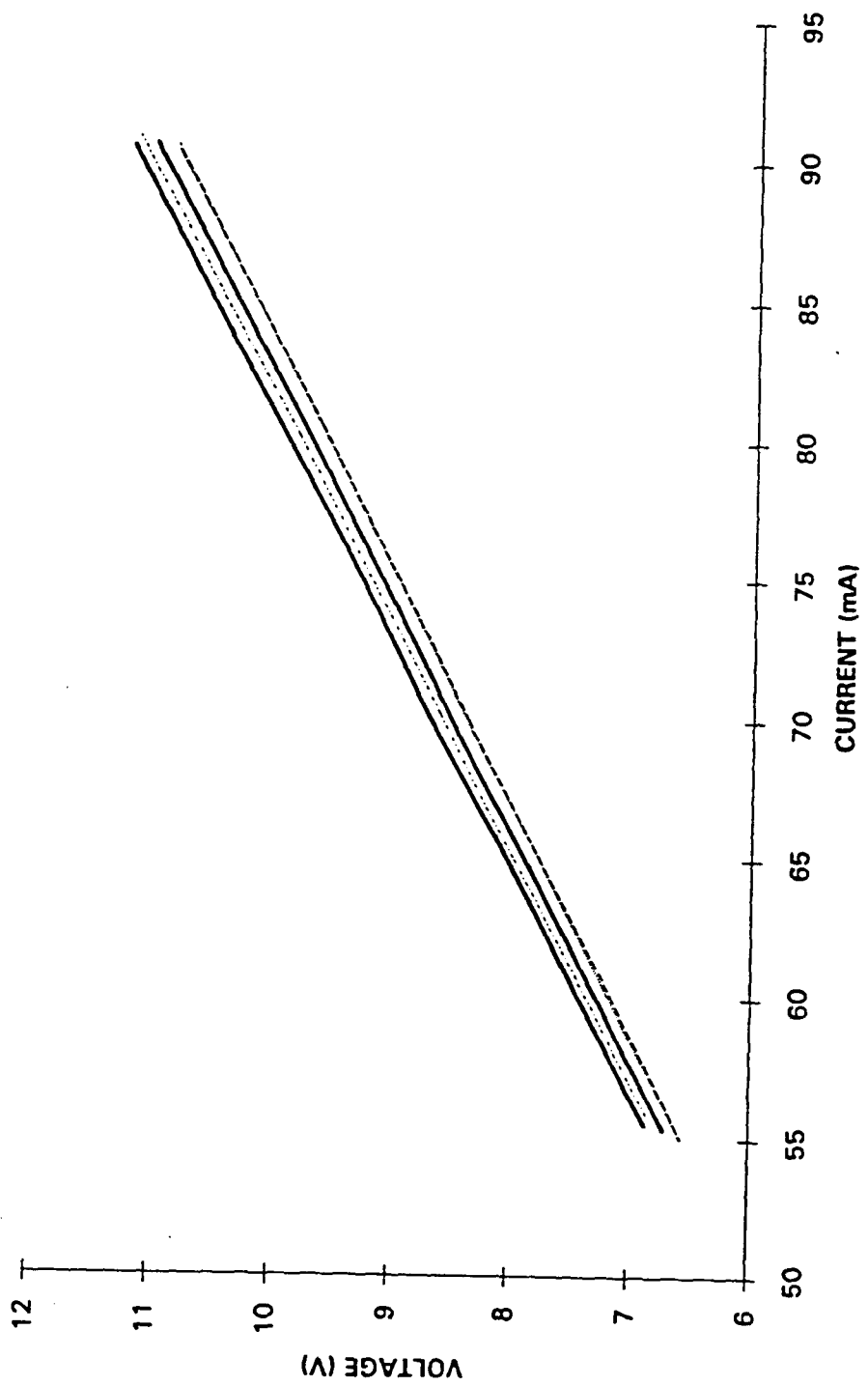
CHAN 22					
I(mA)	V(v)	P(mW)	T(meas)	T(cal)	R (ohms)
55	6.57	361.35	16.5	12.781	119.4545
60.4	7.2	434.88	16.9	13.4666	119.2053
65.7	7.84	515.088	17	13.638	119.3303
70.1	8.36	586.036	17.2	13.9808	119.2582
75.45	9	679.05	17.9	15.1806	119.2843
80.7	9.62	776.334	18.8	16.7232	119.2069
85.7	10.22	875.854	19.9	18.6086	119.2532
90.65	10.81	979.9265	21.2	20.8368	119.2499
AVERAGE RESISTANCE ->					119.2803

CHAN 24					
I(mA)	V(v)	P(mW)	T(meas)	T(cal)	R (ohms)
55.5	6.87	381.285	16.5	12.781	123.7838
60	7.42	445.2	16.7	13.1238	123.6667
65.7	8.1	532.17	16.7	13.1238	123.2877
70.2	8.7	610.74	17.2	13.9808	123.9316
75.9	9.36	710.424	18.2	15.6948	123.3202
80	9.87	789.6	18.8	16.7232	123.375
85	10.49	891.65	20.1	18.9514	123.4118
90.6	11.16	1011.096	21.7	21.6938	123.1788
AVERAGE RESISTANCE ->					123.4944

# 8 TO 12 MICRONS, SUBSTRATE AT 77 K

CHAN 14					
I(mA)	V(v)	P(mW)	T(meas)	T(cal)	R (ohms)
55	6.58	361.9	16.2	12.2668	119.6364
60.6	7.25	439.35	16.5	12.781	119.637
65.4	7.81	510.774	16.6	12.9524	119.419
69.6	8.32	579.072	17	13.638	119.5402
75.6	9.03	682.668	17.6	14.6664	119.4444
80.1	9.56	765.756	18.3	15.8662	119.3508
85.2	10.17	866.484	19.2	17.4088	119.3662
90.5	10.81	978.305	20.6	19.8084	119.4475
95.6	11.42	1091.752	22.2	22.5508	119.4561
100.6	12.01	1208.206	24.3	26.1502	119.3837
106	12.66	1341.96	26.6	30.0924	119.434
111.9	13.37	1496.103	29.9	35.7486	119.4817
115.8	13.83	1601.514	31.9	39.1766	119.4301
120.8	14.43	1743.144	35.5	45.347	119.4536
125.3	14.96	1874.488	38.6	50.6604	119.3935
130	15.5	2015	42.3	57.0022	119.2308
		AVERAGE RESISTANCE ->			119.4441

AVERAGE OF CHANNELS 12, 14, 22, & 24					
I(mA)	V(v)	P(mW)	T(meas)	T(cal)	R (ohms)
55.3425	6.72	371.9508	16.375	12.56675	121.4257
60.4375	7.33	443.0044	16.675	13.08095	121.2823
65.475	7.9325	519.3825	16.775	13.25235	121.1531
70.0375	8.495	594.9995	17.15	13.8951	121.2922
75.505	9.145	690.5088	17.825	15.05205	121.1178
80.2625	9.7125	779.535	18.575	16.33755	121.0092
85.2425	10.32	879.679	19.625	18.13725	121.0664
90.6725	10.975	995.1451	21.1	20.6654	121.04
		AVERAGE RESISTANCE ->			121.1733



8 to 12 Microns, Substrate at 77 K

## **A.V. TEMPORAL RESPONSE DATA**

The tables presented in this section provide the rise times and fall times of resistor elements 16, 17, 19, 24, and 25 based on the 10–90 percent criterion. An example of the measured response in graphical form is given in Figure 12. The measurements were performed with the substrate at ambient temperature. No tests were performed with a cold substrate because of the thermal expansion problems which were identified earlier. As shown in the tables, the rise times varied as a function of input power (column one) with the faster response arising from a higher drive power being applied. Conversely, the fall time increased as more power was applied across the resistor element. From the data, the device demonstrated the ability to respond very fast ( $> 10$  KHz) during the pulse rise interval and, even uncooled, to respond fast enough to support frame rates  $> 2.5$  KHz during the pulse fall interval.

Element: 19, Frequency: 100Hz

Drive Amplitude Vp-p (V)	Detector Voltage Vp-p (mV)	Rise Time (microseconds)	Fall Time (microseconds)
10.94	57.8	92	400
10.16	39.0	106	380
9.22	25.0	100	350
8.59	16.0	95	360
7.8	10.2	120	300
7.03	6.0	140	340
6.40	4.0	150	300
5.62	2.7	200	250
5.0	1.7	150	200

Element: 25, Frequency: 100Hz

Drive Amplitude Vp-p (V)	Detector Voltage Vp-p (mV)	Rise Time (microseconds)	Fall Time (microseconds)
10.78	54	85	400
10.15	35	90	375
9.22	23	95	360
8.59	15.6	140	380
7.81	10.0	150	380
7.18	6.25	130	325
6.4	3.9	250	450
5.78	2.8	400	550
5.0	1.5	120	250

Element: 24, Frequency: 100Hz

Drive Amplitude Vp-p (V)	Detector Voltage Vp-p (mV)	Rise Time (microseconds)	Fall Time (microseconds)
10.78	54	90	360
10.0	38	87	370
9.2	24	100	350
8.44	15.6	100	330
7.75	10.3	120	370
7.03	6.2	150	350
6.4	4.9	200	350
5.62	3.2	250	400
5.0	1.35	400	350

Element: 17, Frequency: 100Hz

Drive Amplitude Vp-p (V)	Detector Voltage Vp-p (mV)	Rise Time (microseconds)	Fall Time (microseconds)
10.78	59	95	395
10.15	37.5	95	370
9.37	25.6	100	370
8.59	16.3	110	340
7.81	10.75	150	400
7.18	6.75	145	350
6.4	4.75	160	400

Element: 16, Frequency: 100Hz

Drive Amplitude Vp-p (V)	Detector Voltage Vp-p (mV)	Rise Time (microseconds)	Fall Time (microseconds)
10.78	59	100	375
10.15	39	90	375
9.37	25.8	110	360
8.59	17.1	105	370
7.81	10.6	125	320
7.18	7	150	350
6.4	4.2	150	310

## **A.VI. CALIBRATION PROCEDURE**

Figure A.1 provides a simple diagram of the experimental setup used to collect the radiometric data which was used for calibration of the temperature data given in column four of the tables presented in Appendix A.I. From the black body based collected data, a linear curve fit was derived which was used to approximate the ideal temperature versus power characteristics of the resistor elements. Using the slope and y-intercept associated with this curve, a two point correction was performed to correlate the IR camera output temperature values for the resistor elements to the ideal black body case. The resultant correction curves are given in Figures A.2 and A.3 for the MWIR and LWIR, respectively. The resulting corrected data are shown in column five of the tables contained in Appendix A.I.

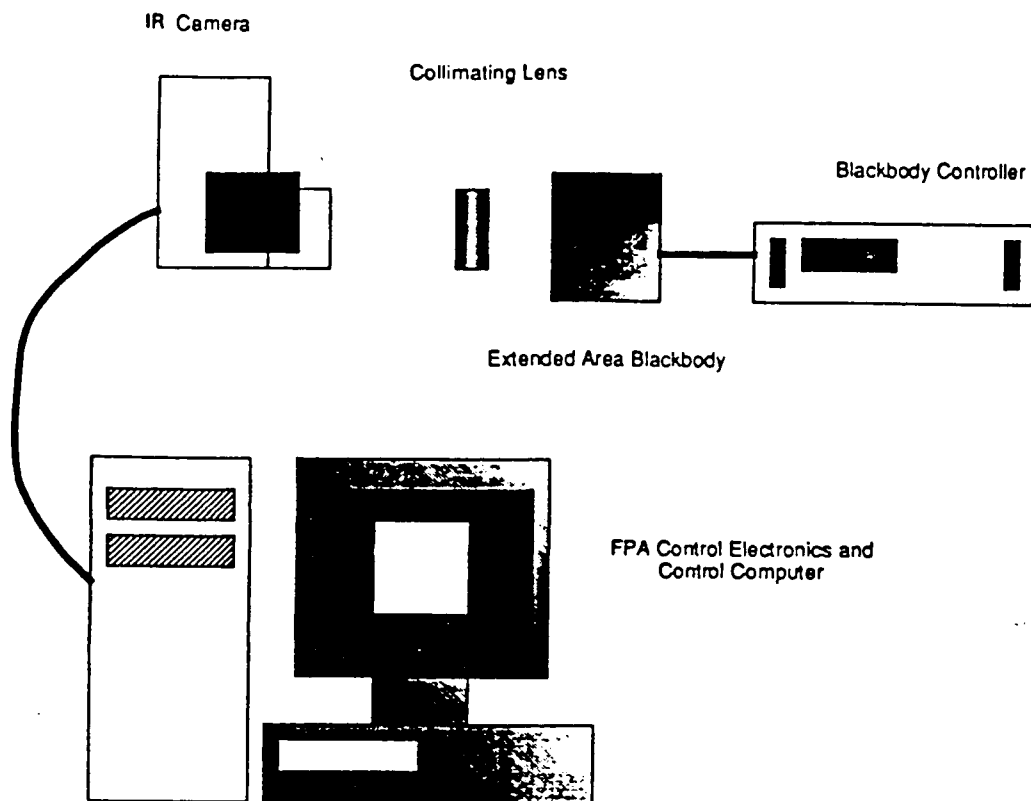


*Figure A-1. IR Camera Calibration Setup*

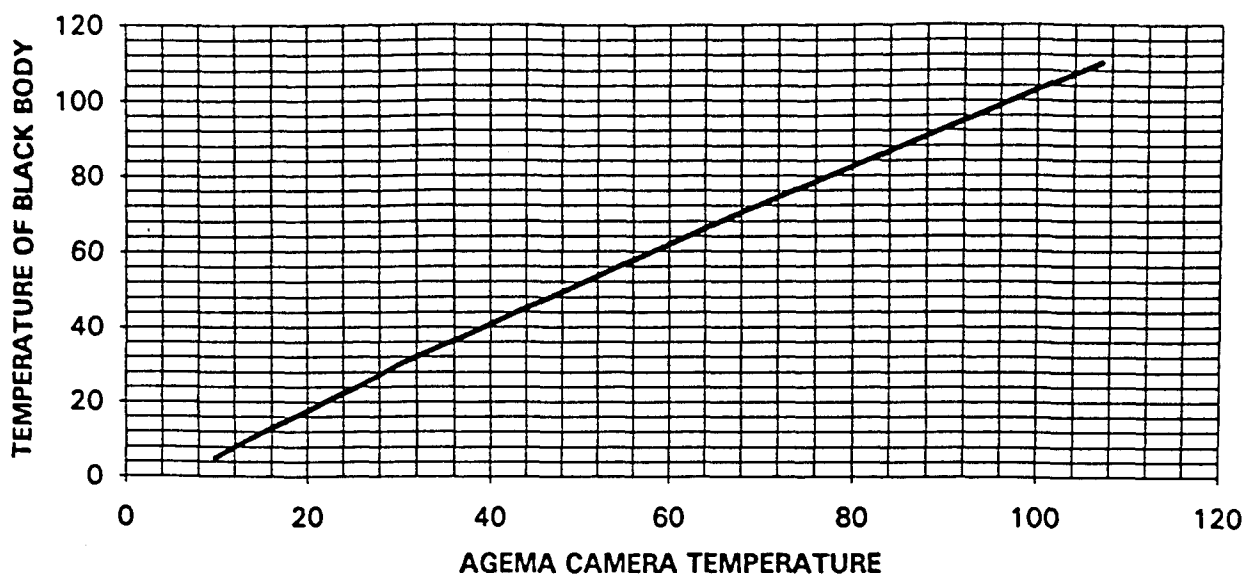


*Figure A-2. MWIR Correction Curve*

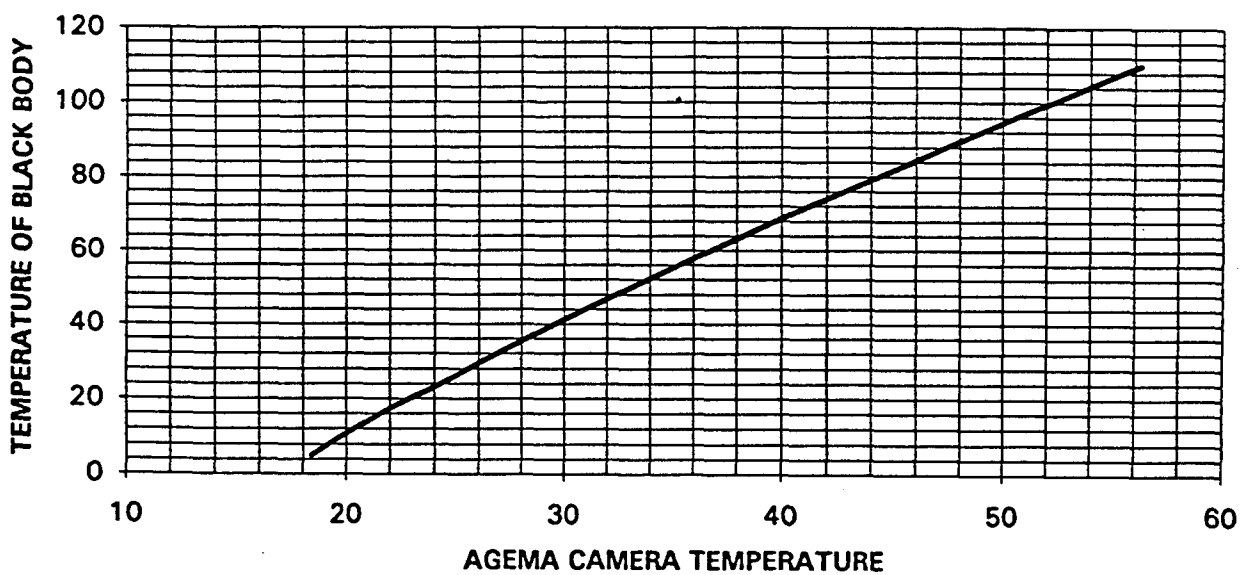


*Figure A-3. LWIR Correction Curve*

**APPENDIX B**  
**DELIVERED TEST DATA**

**APPENDIX B  
DELIVERED TEST DATA**

**RMIT/DSTO Thermal Emitter Arrays**

**Report covering delivery to  
U. S. Army Missile Command**

**1st delivery: December 1993**

**Contributing Agencies:**

- Technisearch Ltd
- Royal Melbourne Institute of Technology
- Defense Science and Technology Organization Australia

## TABLE OF CONTENTS

	<u>Page</u>
<b>1. INTRODUCTION .....</b>	<b>B-4</b>
<b>1.1 Unpacking and Handling .....</b>	<b>B-4</b>
<b>1.2 Pre-Delivery Device Preparation .....</b>	<b>B-4</b>
<b>2. DEVICE DESCRIPTION .....</b>	<b>B-5</b>
<b>2.1 Materials .....</b>	<b>B-5</b>
<b>2.2 Device Fabrication .....</b>	<b>B-6</b>
<b>3. OPERATIONAL CHARACTERISTICS .....</b>	<b>B-8</b>
<b>3.1 Electrical and Thermal Characteristics .....</b>	<b>B-8</b>
<b>3.1.1 Recommended Drive Method .....</b>	<b>B-8</b>
<b>3.1.2 Resistance Variability Compensation .....</b>	<b>B-9</b>
<b>3.1.3 Power Requirement .....</b>	<b>B-10</b>
<b>3.1.4 Heat Sink Requirements .....</b>	<b>B-10</b>
<b>3.1.5 Limiting Performance .....</b>	<b>B-10</b>
<b>3.1.6 Cryogenic Operation .....</b>	<b>B-11</b>
<b>3.2 Infrared Emission Characteristics .....</b>	<b>B-12</b>
<b>3.2.1 Emissivity and Spectral Character .....</b>	<b>B-12</b>
<b>3.2.2 Effective Blackbody Temperature .....</b>	<b>B-12</b>
<b>3.3 Speed of Response .....</b>	<b>B-15</b>

## **1. INTRODUCTION**

In this report, the RMIT/DSTO 2 x 36 thermal infrared emitter arrays delivered to U. S. Army Missile Command (MICOM) in December 1993 are described and operational procedures are defined. Device specifications are included at Attachment A. Note that although the first generation devices in this delivery operate at high speed (10–90 percent risetime 200  $\mu$ s), they do not meet the MICOM speed of response criterion. All other criteria are met. The speed criterion will be met by the second generation devices to follow shortly.

Note also that because the devices are developmental in nature, the specifications, performance levels and quality control procedures are continually being refined. Every effort will be made by DSTO and RMIT to assist with the operation of the devices within MICOM. A listing of the primary supplier contacts is included at Attachment B.

### **1.1 Unpacking and Handling**

While the devices are mechanically robust (with the exception of fine wires connecting between the resistors and the ceramic substrate), sensible levels of care should be taken when they are unpacked, stored and generally handled.

Extreme levels of care must be taken in the vicinity of the wire connects. If visually inspecting the devices under a microscope, particular care must be taken at high magnifications in order to ensure that the microscope objective does not extend into the wire connection region. The wires will be distorted and the bonds will possibly break if they are mechanically disturbed.

Although the devices can be operated successfully in an open laboratory environment, it is advisable to take care to ensure that dust is excluded from the array surface. DSTO operational experience has revealed that during operation dust is electrostatically attracted to the array surface.

If excessive levels of dust accumulate on the array surface, a light stream of nitrogen gas can be used with extreme care to clean the surface. The gas velocity must be sufficiently low to ensure that the wire connections are not physically disturbed.

### **1.2 Pre-Delivery Device Preparation**

After the devices have been received at DSTO from the RMIT manufacturing plant, all pixels are visually checked under a microscope and the resistance values across the array are read and recorded. Devices with visible defects or individual resistance values lying outside an acceptable spread (generally  $\pm 2$  ohms) have generally been rejected by RMIT during prior pre-delivery checks.

All resistors are then operated for a short period during a 'burn-in' procedure which provides an annealing function at the resistor/insulator interface. After burn-in, the resistance values are again recorded on a test certificate that accompanies each device. The arrays are then in a state where they can be operated within specification.

Note that the devices are still at a developmental stage, the pre-delivery procedures still being in a state of refinement and extension. In future deliveries, it is intended that each array will have been checked for infrared signal radiance capability against an imaging

radiometer. Currently, spot measurements of infrared radiance from individual pixels define the extent of the pre-delivery check.

## 2. DEVICE DESCRIPTION

### 2.1 Materials

The arrays are fabricated on a silicon substrate, chosen for its well characterized physical and electrical properties, high thermal conductivity and for its widespread use within the microelectronics industry. The incorporation of on-chip electronic driving circuitry remains a useful future option. The silicon wafer on which array layers are built can be easily cleaved or sawn, allowing a number of devices to be obtained as a batch from the one wafer.

The infrared emitting elements are comprised of electrically heated thin-film resistors. Although it is possible to fabricate the resistors directly on the surface of the silicon substrate, the power requirements would be excessive even for individual element operated only a few degrees above ambient temperature. Such an approach would place a serious limitation on array size.

The drive power limitation can be partially overcome by using a thin thermally and electrically insulating layer sandwiched between the substrate and the resistive elements. For such a purpose, materials such as  $\text{SiO}_2$  or  $\text{Si}_3\text{N}_4$  are unsuitable since the thermal conductivities, while being around 1 percent of that of silicon, are still incapable of providing the necessary thermal insulation unless excessively thick layers are used. Materials such as polyimides are preferred since they tend to be characterized by thermal conductivities of the order of 0.1 percent of that of silicon. It is found that polyimide layers at around 5 – 10  $\mu\text{m}$  thickness provide thermal isolation sufficient to reduce the drive power requirement to a reasonable level.

A single element consists of a rectangular resistor measuring 330  $\mu\text{m}$  x 320  $\mu\text{m}$  within a 360  $\mu\text{m}$  x 360  $\mu\text{m}$  pixel area (fill factor 81 percent). The array is fabricated in the form of two rows of 36 elements, the rows being connected by a common central busbar. The pixel plan view and cross-section are sketched in Figure 1.

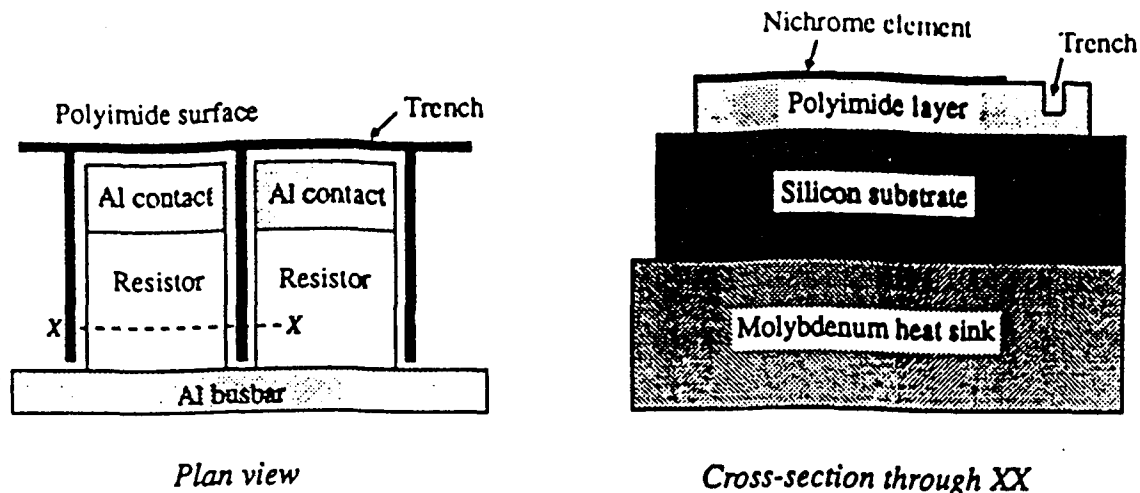
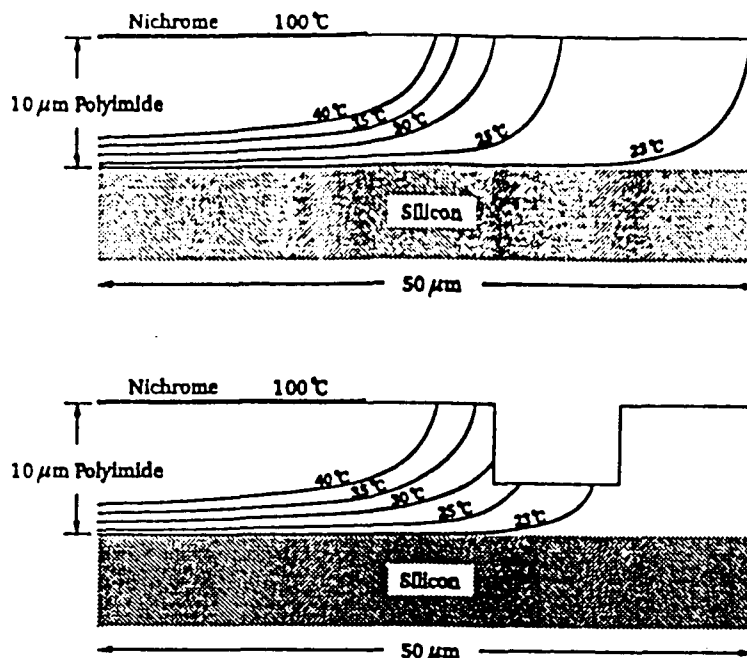


Figure 1. Pixel Views

Each element in the array is separated from its neighbor by a narrow trench etched into the polyimide, the purpose of the trench being to reduce the thermal crosstalk between adjacent resistive elements. The effect of this trench on lateral (and longitudinal) heat transfer has

been calculated using a two dimensional finite element thermal analysis technique. The results of the analysis are shown in Figure 2 where isotherms in the presence and absence of the trench (6  $\mu\text{m}$  deep x 10  $\mu\text{m}$  wide) are depicted. The presence of the polyimide trench causes a more abrupt change in temperature towards the edge of each emitting element. It is clear that there is little more to be gained by increasing the depth of the trench.



*Figure 2. Steady State Isotherms for Thin-Film Resistor Arrays  
(with and Without Isolation Trench)*

It is necessary that the thin-film resistive element on the surface be characterized by a reasonably high value of sheet resistance since otherwise the current requirement for the required level of drive power becomes excessively high. This can lead to problems with interconnection design and bonding wire current carrying capacity. The resistive film should also be suitable for deposition in a thin-film form (by sputtering or vacuum evaporation).

In the present array design, the elements are fabricated use NiCr metallization, the individual elements being patterned by wet chemical etching. The nichrome passivates in air forming a thin oxide layer which assists in resistor stabilization.

## 2.2 Device Fabrication

The array fabrication process is conducted using two inch diameter silicon wafers at about 400  $\mu\text{m}$  thickness. Polyimide films deposited onto the silicon wafer are subsequently etched to provide the thermal isolation trenches in the polyimide. The polyimide is then fully cured before a 10 – 20 nm of nichrome is deposited to form the resistive surface layer.

The interconnection path and the resistive element contact pads are formed by evaporating several microns of aluminium onto the nichrome. This process is followed by photoresist patterning and etching of both the aluminium and the nichrome in order to form the individual resistor elements. At this stage of the fabrication the elements may be probed in an initial check on resistance, allowing arrays that lie outside the resistance specification range to be rejected. The arrays on the wafer are finally separated either by diamond sawing or scribing. A photograph illustrating part of an array is shown in Figure 3.

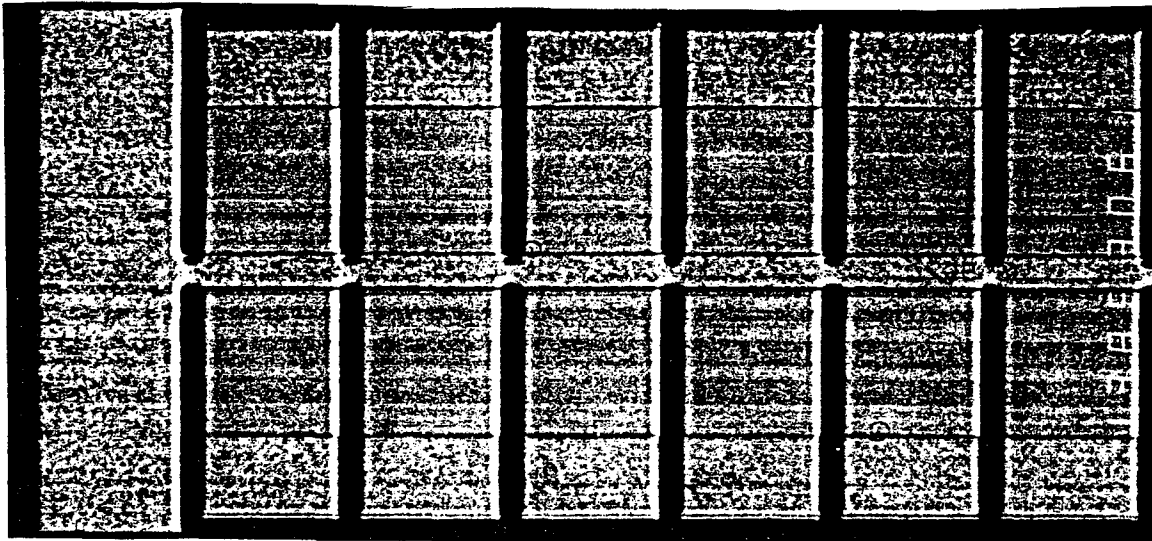


*Figure 3. Partial Plan View of Array*

The silicon chip on which the array has been fabricated is mounted on a gold plated molybdenum heat sink which is in turn attached to an alumina interconnect substrate measuring 2 inch x 2 inch.

Metallized interconnections run from the edge of the substrate up to the edges of a central rectangular hole cut into the substrate. The thermal array is mounted within this central hole. Wire bonding completes the electrical connections. The alumina substrate and its interconnections are shown in Figure 4 and a completed device (not in the special MICOM form) is shown in Figure 5. Note that early in 1994, devices will be available in a new computer-chip style package with dual pin grid arrays that mate to a standard socket.

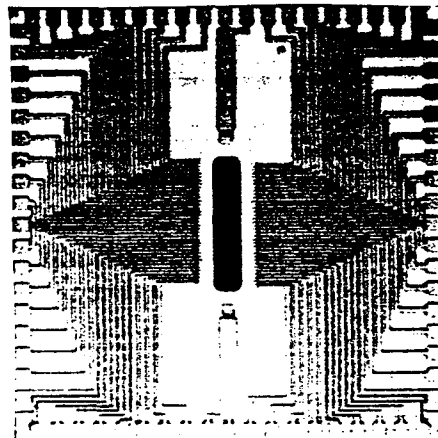


*Figure 4. Alumina Substrate and Interconnections*

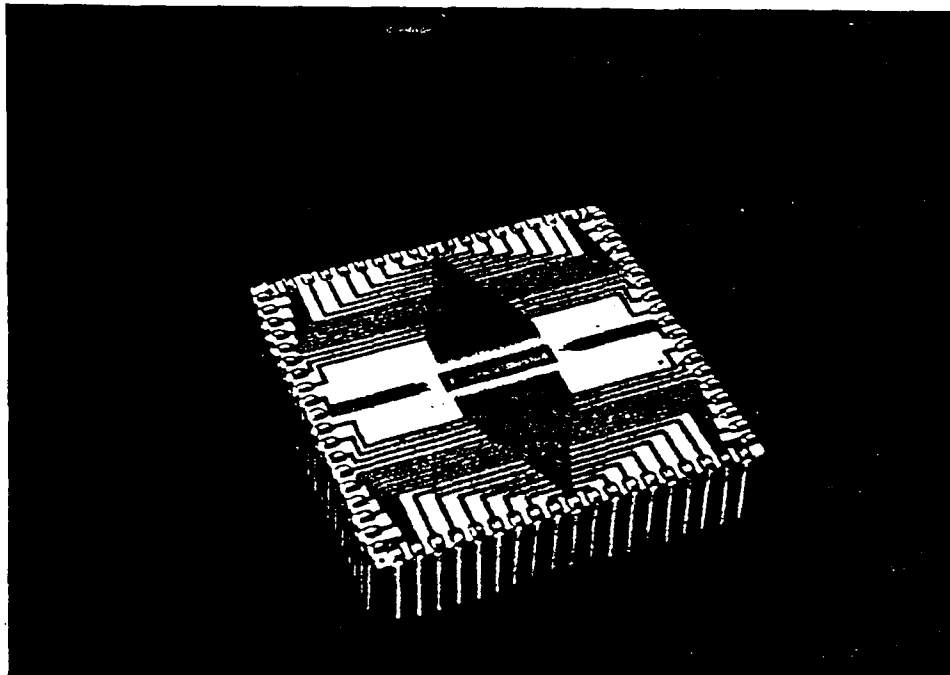


*Figure 5. Complete Device (with External Pins)*

### 3. OPERATIONAL CHARACTERISTICS

#### 3.1 Electrical and Thermal Characteristics

##### 3.1.1 Recommended Drive Method

Each element in the array is an ohmic surface resistor occupying  $320 \times 330 \mu\text{m}^2$  area (fill factor = 81 percent) within the  $360 \times 360 \mu\text{m}^2$  pixel area. In the present design, element resistance is typically  $125 \pm 2$  ohms, the variability being caused by microscopic undulations in the polyimide layer on which the 20 nm nichrome resistive layer is deposited. In occasional devices, one or more elements may lie outside of the general range of variability due to the presence of more pronounced local variations in the polyimide surface texture. Note that the inter-device resistance variability can be greater than the intra-device resistance variability quoted above (because of macroscopic variations across the wafer). Each device is supplied with a test certificate in which all resistance values measured prior to shipping are listed.

Since the resistors are ohmic in character, all standard methods of driving ohmic loads are saltable, within the power constraints designated below. As a result of the variation in resistance values across the array, it is recommended that in Dynamic Infrared Scene Projection (DIRSP) applications the resistors be addressed through a computer where appropriate compensation techniques can be applied in order to minimize the effect of the variability. Refer to Section 3.1.2 below.

DSTO operational experience has also identified the characteristic that the resistance values change slowly as the elements are operated, particularly when high drive powers are used. The resistance change is slow compared to the time of most DIRSP experiments. It is therefore recommended that the resistance values across the array be read into the addressing computer memory prior to each run in order to ensure that the resistance variation compensation calculations can be updated.

### 3.1.2 Resistance Variability Compensation

In order to compensate for the range of resistance variability it is recommended that the resistors be operated in a constant power mode, consistent with the fact that the applied power is (almost exclusively) dissipated by thermal conduction through the polyimide insulation to the silicon substrate and thence to the heat sink. Hence, since

$$\dot{Q} = k A_c \frac{\Delta T}{\Delta x}$$

the rise  $\Delta T$  in surface temperature is proportional to the applied power. Note that the effective blackbody temperature difference

$$\Delta T_{\text{eff}} = T_{\text{eff}} - T_s = \Delta T_{\text{eff}}(\Delta T, g_a)$$

(where  $T_s$  is the sink temperature) is a function of  $\Delta T$  and of  $g_a$ , the latter parameter being defined as the active zone attenuation coefficient which accounts for the cumulative emission losses. Since  $g_a$  is constant within a given Infrared Scene Projection (IRSP) application, a constant power mode of operation will therefore be successful in generating a constant level of effective blackbody temperature.

Given the variations across the array, it is recommended that the array resistances be recorded and the values updated from time to time. Once the power level

$$P = \frac{V_o^2}{R_o}$$

required to achieve a given level of  $T_{\text{eff}}$  in the desired IRSP application has been established for a reference resistor  $R_o$  (by thermal imaging or other methods), then the applied voltage distribution required to achieve a common value of power and hence of  $T_{\text{eff}}$  across the array may easily be calculated from the resistance distribution as

$$V = V_o \left( \frac{R}{R_o} \right)^{\frac{1}{2}}.$$

Since the relationship between applied voltage  $V_o$  and  $T_{\text{eff}}$  is nonlinear, it is recommended that for each IRSP system a look-up table be generated across the required range of effective blackbody temperatures.

It is clearly desirable in an IRSP application that the array be addressed through a computer, enabling the look-up table to be used together with simple compensation software based on the above formula, enabling a corrected distribution of drive voltages to be delivered to the array.

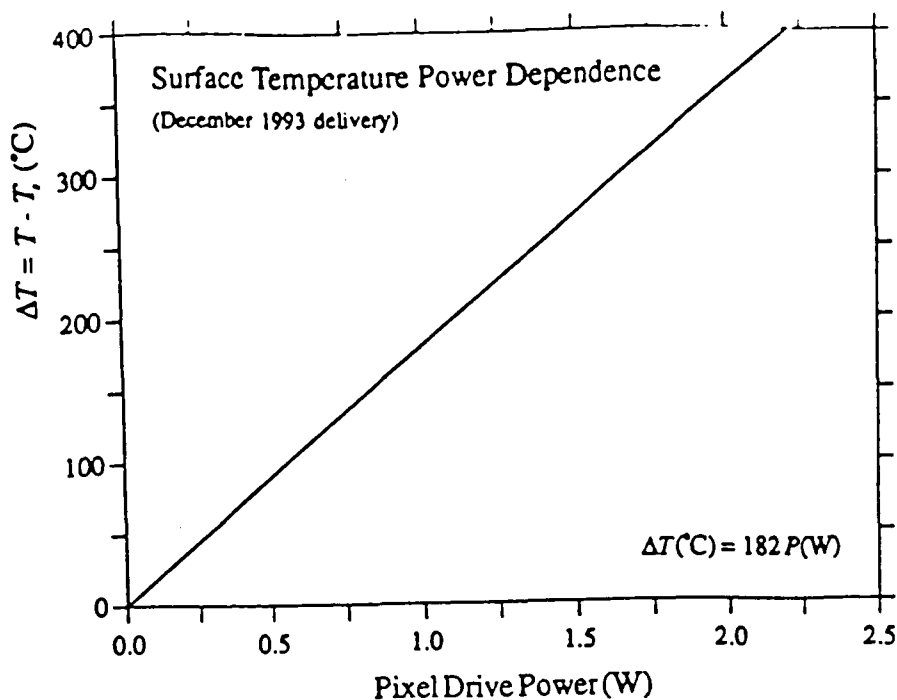


Figure 6. Surface Temperature Power Dependence

### 3.1.3 Power Requirement

Power requirement for the first delivery devices (December 1993) is 5.5 mW/pixel per degree Celsius temperature difference between the emitting surface and the heat sink.

Note that the second delivery devices (early 1994) capable of higher speed operation will be characterized by a higher power requirement (expected to be around 8 mW/pixel/°C).

### 3.1.4 Heat Sink Requirements

It is regarded as critical that the arrays are always operated in good thermal contact with a well-designed heat sink capable of removing heat as it is generated.

Without this precaution, hot regions can develop both in the vicinity of resistors that are being operated at high temperatures and along the central busbar carrying the return current. Normal practices of thermal heat sink design should always be adopted.

The arrays have not been designed to be operated under conditions where many pixels are driven simultaneously to high temperatures for extensive periods.

It is, however, possible to operate single pixels at high temperatures for extended periods or a number of pixels simultaneously at high temperatures for short periods (for example, for a few seconds). In essence, the high temperature IR capability is only available for point target simulation or for extended target simulation over short periods, such as might occur during the endgame phase of a simulated air-to-air missile engagement.

### 3.1.5 Limiting Performance

The resistor elements consist of a mere 20 nm of nichrome deposited on a polyimide insulation layer and at high power levels are subject to strong thermal, electrical, and mechanical stresses. Improvements in the fabrication technology in order to extend the device operational range is an ongoing process. Considerable R&D effort has been expended in order to

identify the drive power limitations and to improve device robustness. The devices that have been delivered to MICOM incorporate the most recent advances in the fabrication technology.

Regardless of the improvements, there is always a power beyond which individual elements fail. Element failure under high power loads has been investigated during extensive destructive testing experiments. The predominant mechanism for long-term device failure has been identified as electromigration. In this process, individual nickel and chromium atoms migrate differentially under the influence of the high electric fields, leading to a weakening of the nickel-chromium alloy structure. The failure mechanism appears to occur predominantly at the nichrome/polyimide interface where presumably the highest stresses occur. Single element failures have been recorded using a microscope/video camera combination and have revealed that failure occurs in regions where a 'hot-spot' develops, identified by a localized browning of the surface. The resulting stresses culminate suddenly in a development of a stress fracture crack that extends across the width of the element and which open-circuits the element.

At very high surface temperatures approaching 400 °C, device failure is more sudden as the polyimide starts to decompose. However, it appears that the devices can withstand such temperatures for short times during a pulsed mode of operation. Experiments designed to identify the range of pulsed operation are continuing.

The destructive testing experiments combined with life-cycle experiments where individual elements are powered to different levels and are periodically switched on and off have been useful in identifying the useful long-term range of operation. It has been found that:

For long-term operation under steady-state conditions, single pixels within the first generation devices delivered to MICOM (December 1993) should not be operated above surface temperatures of about 200 °C, corresponding to a pixel power level of 1 W from an ambient temperature base.

Under pulsed conditions where the pulse duration is significantly smaller than the frame rate (small mark/space ratio), individual elements may be powered to much higher levels (typically, up to 2 W from an ambient temperature base). Pulsed operation experiments are incomplete. Results will be forwarded as they become available.

### 3.1.6 Cryogenic Operation

The thermal emitter arrays delivered to MICOM have been designed for operation at temperatures as low as 77 K. The molybdenum spacer between the silicon substrate and the aluminum mounting pad has been selected in order to minimize differences in thermal expansion. The devices have survived complete immersion in liquid nitrogen. However:

Under no circumstances should water vapor be allowed to condense or freeze on the array surface. Under such conditions, the surface structure will fracture. When operating under any conditions such that the substrate temperature is lower than the dew point temperature, due care must be taken to ensure that moist air is excluded from the vicinity of the thermal emitter array until such time that ambient temperature conditions are re-established.

Operation under cryogenic heat sink conditions will necessarily lead to higher power demands, both to simulate the specified ambient temperature and to simulate targets at temperatures higher than ambient. The power requirement for the MICOM devices is 5.5 mW/pixel per degree Celsius surface temperature difference. Cryogenic operation has the advantage that the emissions from the inactive pixel regions (polyimide trenches, Al central busbar) will be reduced to insignificant levels. In contrast, emissions from the inactive regions will be observed when an array connected to an ambient temperature heat sink is viewed with a thermal imaging camera. It is desirable then that the IRSP optical system be designed appropriately in order to obscure spurious infrared radiance reflected from the aluminum busbar.

## 3.2 Infrared Emission Characteristics

### 3.2.1 Emissivity and Spectral Character

The design formula has been improved to the stage whereby the resistor elements in the devices delivered to MICOM are gray-body emitters characterized by an emissivity close to unity. Emissivity has been determined by comparing measurements of surface temperature verses drive power with corresponding measurements of effective blackbody temperature verses power.

The surface temperature measurements were conducted observing the power levels at which a series of microcrystals of known melting points melted on the heated resistor elements. Effective blackbody temperature measurements as a function of power were conducted by viewing 4 – 5  $\mu\text{m}$  collimated radiance from an individually heated pixel using an infrared radiometer and comparing the signal voltage per unit source area with that generated when the measurements were repeated using a blackbody source and calibrated aperture plate. The comparison procedure yielded an emissivity of  $0.95 \pm 0.05$ . This high emissivity value is to be confirmed through independent measurements to be conducted shortly using bulk thin-film material. Results will be forwarded to MICOM as they become available.

Spectral measurements of single pixel radiance have confirmed the gray-body nature of the emission. Projected array radiance has also been viewed using a dual-band thermal imager operating in both the MWIR and LWIR infrared transmission bands.

### 3.2.2 Effective Blackbody Temperature

As noted above, effective blackbody temperature difference

$$\Delta T_{\text{eff}} = T_{\text{eff}} - T_s = \Delta T_{\text{eff}} (\Delta T, g_a)$$

is a function of the actual temperature difference  $\Delta T = T - T_s$  and the *active zone attenuation coefficient*  $g_a$ . At low temperature differences

$$\Delta T_{\text{eff}} = g_a \Delta T.$$

For emissive projectors,  $g_a$  equals the product

$$g_a = \epsilon_a \phi_a \bar{\tau}_p$$

of the factors that contribute to attenuation of infrared signal radiance: the active (heated) zone emissivity  $\epsilon_a$ , the geometric fill factor  $\phi_a$  and the transmission coefficient  $\bar{\tau}_p$  of the projector optics (averaged appropriately over the spectral band of interest). For the devices supplied to MICOM,  $\epsilon_a = 0.95$  and  $\phi_a = 0.81$ , while the value of  $\bar{\tau}_p$  must be estimated appropriate to the specific IRSP optics used to connect the device with the unit-under-test.

The functional forms of  $\Delta T_{\text{eff}}$  have been calculated and are displayed in Figures 7 to 10, covering both the MWIR (3 – 5  $\mu\text{m}$ ) and LWIR (8 – 12  $\mu\text{m}$ ) bands and heat sinks held both at ambient temperatures and at the boiling point of liquid nitrogen. Data corresponding to other heat sink temperatures can be supplied on request.

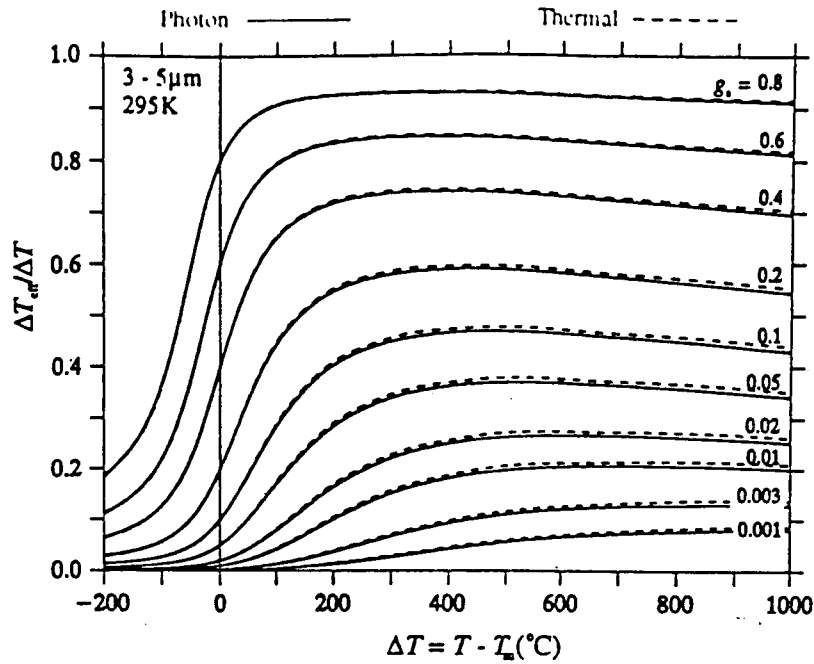


Figure 7. Effective Blackbody Temperature Difference (3 – 5  $\mu\text{m}$ ,  $T_{su} = 295 \text{ K}$ )

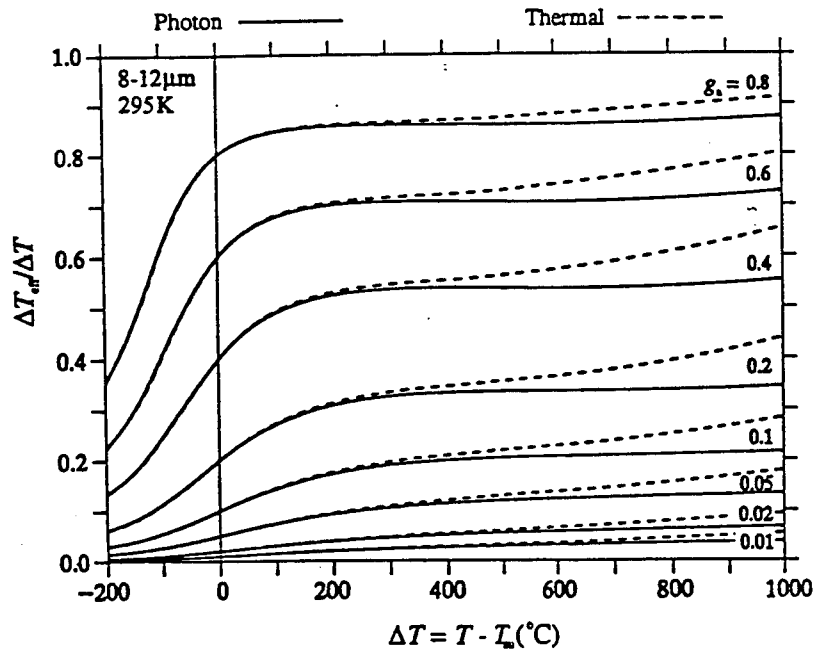


Figure 8. Effective Blackbody Temperature Difference (8 – 12  $\mu\text{m}$ ,  $T_{su} = 295 \text{ K}$ )

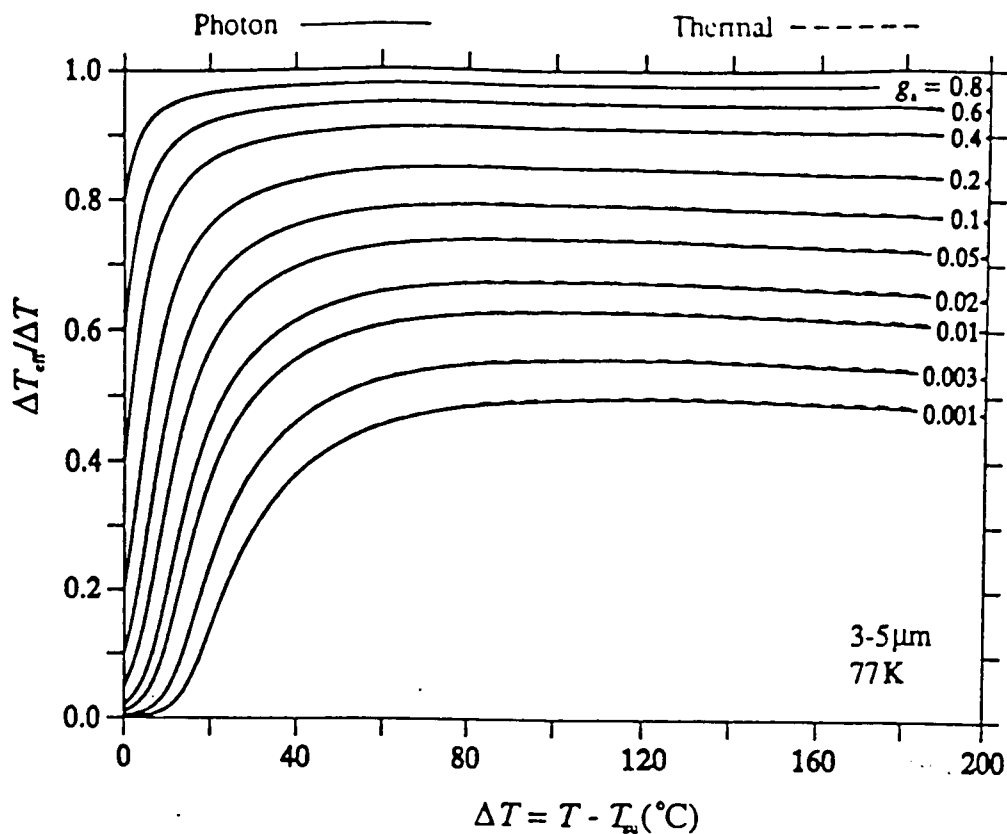


Figure 9. Effective Blackbody Temperature Difference (3 – 5  $\mu\text{m}$ ,  $T_{su} = 77\text{ K}$ )

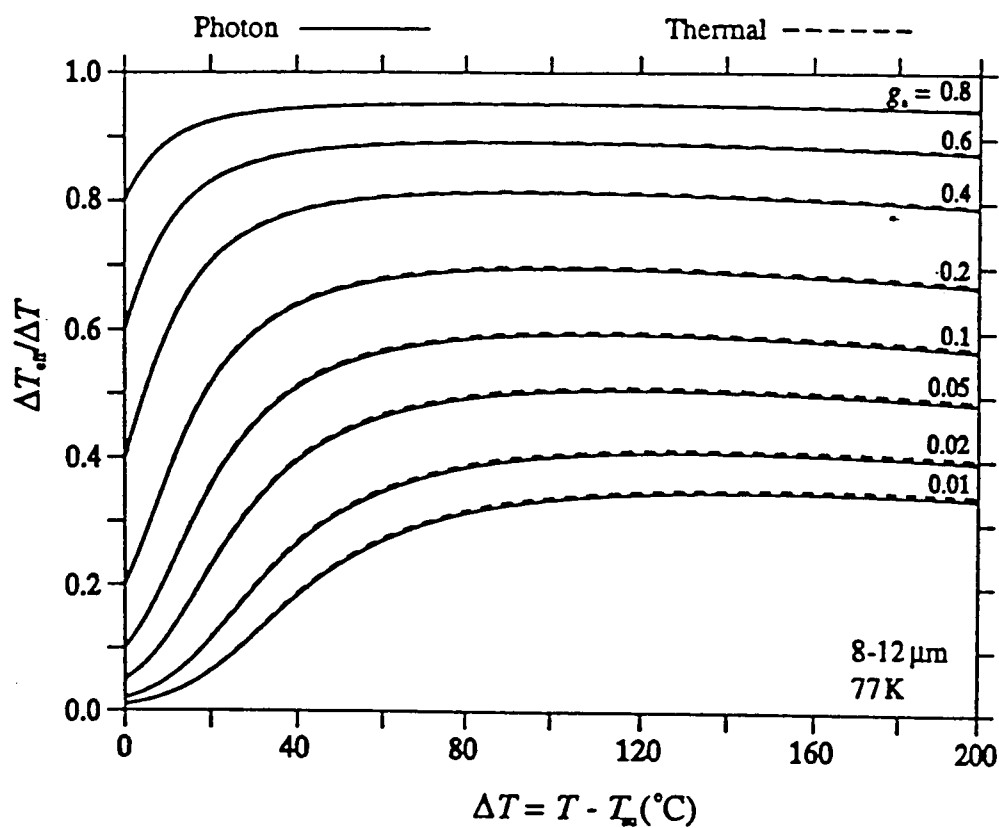


Figure 10. Effective Blackbody Temperature Difference (8 – 12  $\mu\text{m}$ ,  $T_{su} = 77\text{ K}$ )

### 3.3 Speed of Response

Speed of response is determined by the diffusion length and thermal diffusivity of the polyimide insulation layer. As with all emissive projection devices a strong trade-off exists between drive power and device speed. The smaller the polyimide depth, the smaller both the length of the heat conduction path and the thermal diffusion length; hence, both power and speed are higher. Drive power is reduced proportionate to the increase in insulation depth while the speed of response is inversely proportional to the square of the insulation depth.

The initial delivery to MICOM has been based on a compromise design in which speed of response (10–90 percent risetime  $\sim 200 \mu\text{s}$ ) is sacrificed in order to maintain drive powers at a moderate level (5.5 mW/pixel per degree Celsius surface temperature difference). The devices in the second delivery (early 1994) will be characterized by higher speed (10–90 percent risetime  $\sim 100 \mu\text{s}$ ) at the expense of higher drive power ( $\sim 8 \text{ mW/pixel}$  per degree Celsius surface temperature difference).

Projector speed capability in following the demands for updated scene information (e.g., as a scene is panned across the field-of-view of an imaging UUT) needs to be assessed in terms of the rate at which the radiance can be changed. The speed of response of emissive infrared projectors tends instead, however, to be governed by the rate at which the temperature changes. It is therefore necessary to compare the temperature and infrared signal transient responses.

At small signal levels there is little difference between signal and temperature response since signal radiance is to a good approximation proportional to temperature difference  $\Delta T$ . However, as the temperature demand is increased the signal radiance rises at an increasingly rapid rate in accordance with the joint nonlinear effects of the  $T^4$  increase in radiated power and the shift of the Planck spectral maximum towards shorter wavelengths. The incremental changes in infrared signal radiance as the demanded temperature is approached therefore exceed the complementary changes in temperature, the consequence being that the rising signal response is slower than the rising temperature response. The opposite effect occurs on for falling signal levels, consistent again with the expectation stemming from the temperature dependence of the Planck blackbody spectrum.

In order to illustrate this effect, the relevant responses to a rectangular pulse demand are shown in Figure 11, the data for which have been derived by appropriate application of in-band blackbody signal radiance/temperature data. It is noted in passing that it is possible to improve the signal risetime by overdriving the emissive element for a time immediately following the increased temperature demand, but only at the expense of increased addressing scheme complexity.

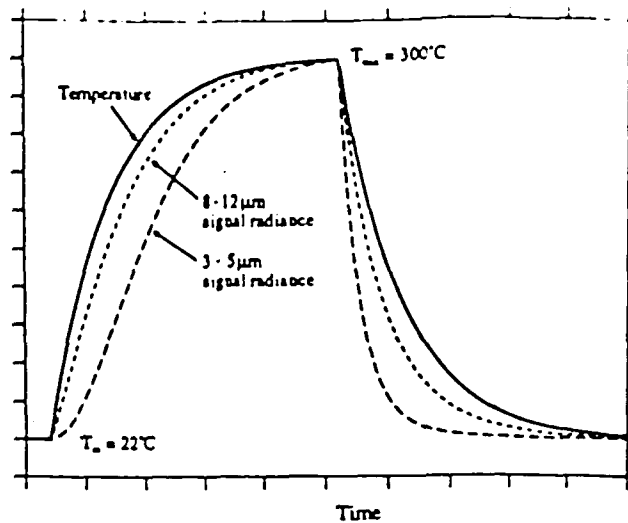


Figure 11. Transient Responses of Temperature and Signal Radiance to a Rectangular Pulse Demand

Rise and fall time data covering the range of operational temperatures have for convenience been collated in Figure 12. Here, the times taken for both temperature and signal to rise to 90 percent, 99 percent, and 99.9 percent of the demanded value are shown together with the times taken for the corresponding decay process (all assuming exponential temperature changes). Note that the differences between the values calculated for the signal and temperature rises are not as great across the temperature range as might have been expected. It appears that for many IRSP experiments an acceptable speed criterion would be to allow 5–6 time constants for both the temperature and infrared signal to settle towards their intended values.

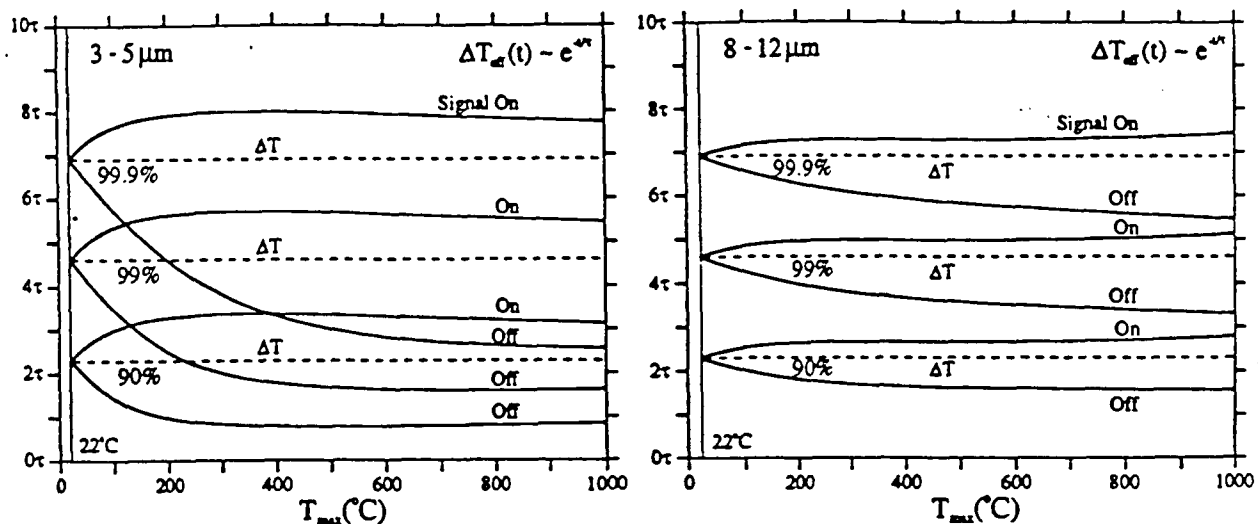


Figure 12. Emissive Projectors: Times Required to Change by Designated Percentages

Specific responses of the first delivery MICOM devices (December 1993) to a rectangular drive pulse, as recorded using an InSb photodiode detector, are shown in Figure 13 and the measured MWIR 10–90 percent rise and fall times are shown in Figure 14.

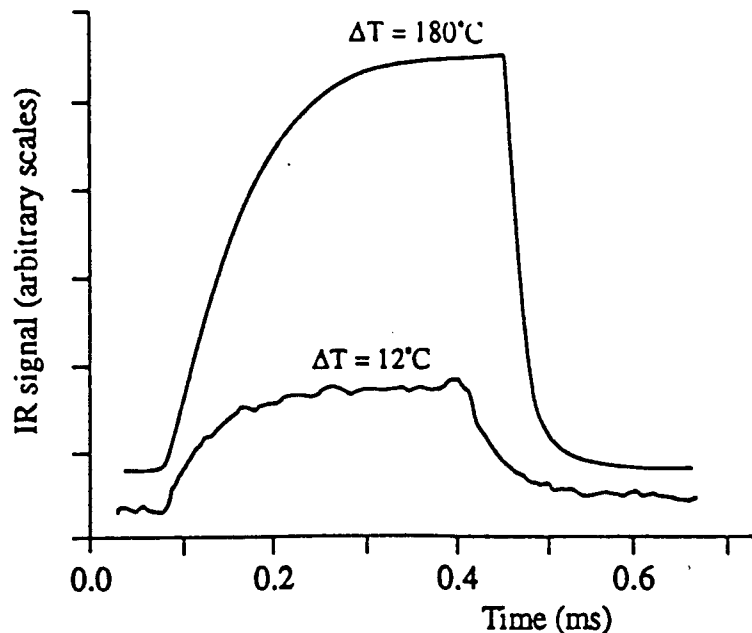


Figure 13. Measured Pulse Responses

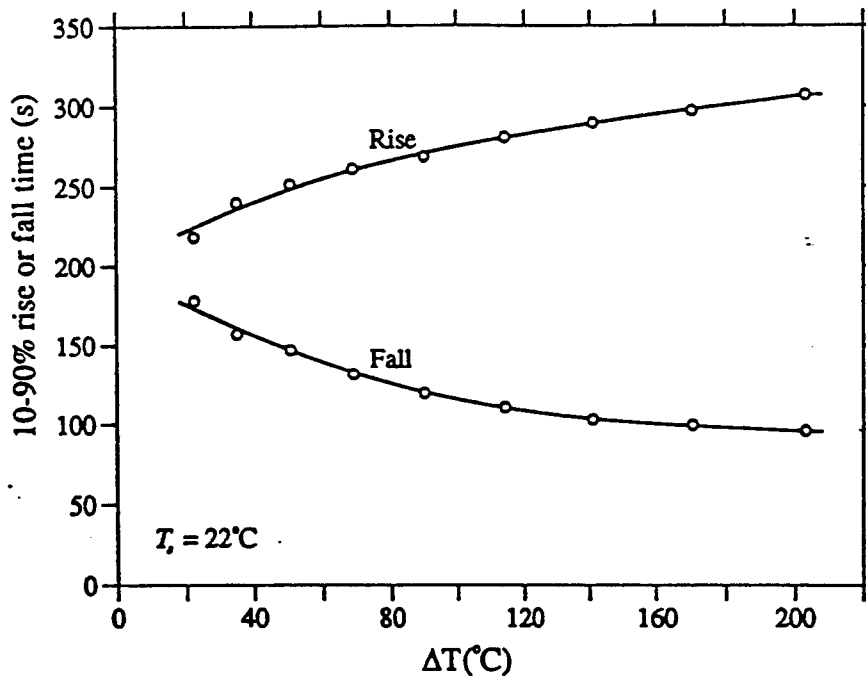


Figure 14. Measured MWIR Signal Rise and Fall Times

## Device Specifications

Properties	
<i>Physical</i>	
Array size	2 × 36
Pixel size	360 × 360 $\mu\text{m}^2$
Element size	330 × 320 $\mu\text{m}^2$
Packaging	2 inch × 2 inch ceramic substrate with flying leads
Insulation material	Polyimide
Resistor material	Nichrome
Cryogenic capability	yes
Vacuum capability	yes
Temperature range	77 – 500 K steady-state drive 77 – 600 K pulsed drive
<i>Electrical</i>	
Element resistance	125 $\Omega$ nominal
Array tolerance	$\pm 1 \Omega$ 1 standard deviation
Batch range of variation	120 – 130 $\Omega$
Array reference mark	top left corner
10-90% risetime	100 – 300 $\mu\text{s}$
Power requirement	5.5 mW $^{\circ}\text{C}^{-1}$ pixel $^{-1}$ insulation depth dependent $\sim 8 \text{ mW } ^{\circ}\text{C}^{-1}$ pixel $^{-1}$ December 1993 delivery 1994 deliveries (high speed)
Maximum recommended power	1 W/pixel continuous from ambient temperatures $\sim 2 \text{ W/pixel}$ pulsed @ low mark/space ratio
Maximum recommended bus current	500 mA continuous
Addressing scheme	direct hard wired
<i>Infrared</i>	
Spectral range	MWIR + LWIR
IR window	none
Geometric fill factor	81%
Emissivity	95 $\pm$ 5% MWIR
$T_{\text{eff}}$ range	77 – 450 K @ $g_a = 0.6$ ; steady-state drive
Effective thermal capacity, $C_{\text{eff}} = \dot{Q}/\Delta T_{\text{eff}}$	8 – 16 mW $^{\circ}\text{C}^{-1}$ pixel $^{-1}$ @ $g_a = 0.6$ insulation depth dependent
<i>Thermal</i>	
Heat sink	essential Mo back plate/Al mounting pl.
Effective heat transfer coefficient, $h_{\text{eff}} = C_{\text{eff}}/A_{\text{px}}$	6 – 12 W $\text{cm}^{-2} ^{\circ}\text{C}^{-1}$ @ $g_a = 0.6$
Thermal time constant	30 – 100 $\mu\text{s}$ insulation depth dependent

## **LIST of CONTACTS**

### **Business Matters**

Mr Malcolm Mulcare  
Manager-Industrial Consulting Unit  
Technisearch Ltd  
PO Box 1457  
Collingwood VIC 3066  
Australia  
*Telephone:* (Int) +61 3 483 6560  
*Facsimile:* (Int) +61 3 419 4529  
*e-mail:* malcolm@tsmain.ts.rmit.edu.au

### **Device Design and Fabrication**

Dr Geoffrey K. Reeves  
MMTC  
Royal Melbourne Institute of Technology  
GPO Box 2476V  
Melbourne VIC 3001  
Australia  
*Telephone:* (Int) +61 3 660 3073  
*Facsimile:* (Int) +61 3 662 1921

### **Device Evaluation and Dynamic Infrared Scene Projection**

Dr Owen M. Williams  
Guided Weapons Division  
DSTO Salisbury  
PO Box 1500  
Salisbury SA 5108  
Australia  
*Telephone:* (Int) +61 8 259 5590  
*Facsimile:* (Int) +61 8 259 5688  
*e-mail:* omw@dstos3.dstos.gov.au



Technisearch

# 2 x 36 INFRARED EMITTER ARRAY TEST DATA SHEET



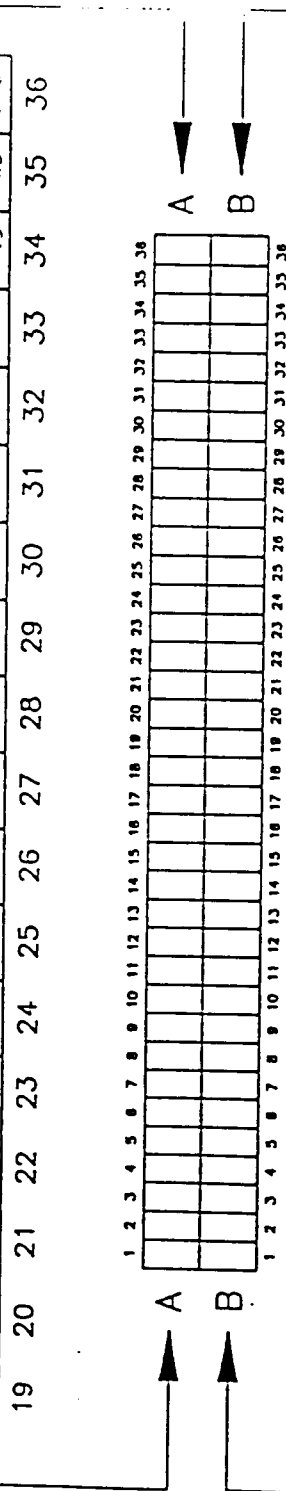
Element Resistance (ohms)

Serial Number: 93171-1

123.7	123.7	123.6	123.9	123.7	123.0	123.7	124.8	o/c	124.1	124.0	123.7	123.6	124.2	124.0	124.1	123.4
-------	-------	-------	-------	-------	-------	-------	-------	-----	-------	-------	-------	-------	-------	-------	-------	-------

Row A

19	20	21	22	23	24	25	26	27	28	29	30	31	32	33	34	35	36
124.3	123.7	123.9	125.1	123.7	123.1	123.7	123.7	124.3	124.6	124.3	123.7	123.6	123.2	122.7	121.5	121.5	121.6



1	2	3	4	5	6	7	8	9	10	11	12	13	14	15	16	17	18
123.0	121.4	124.6	121.1	122.7	123.5	123.5	124.0	124.6	124.3	124.4	124.4	123.7	123.4	123.8	123.8	124.0	123.6

Row B

19	20	21	22	23	24	25	26	27	28	29	30	31	32	33	34	35	36
123.7	123.7	123.7	123.7	123.8	123.7	123.7	123.7	123.7	124.1	124.1	124.1	124.0	123.6	123.0	121.5	121.3	121.4

Test Officer.....*S. Elgar*

Date...*6/12/93*

R5-419



Technisearch

2 x 36 INFRARED EMITTER ARRAY



# TEST DATA SHEET

Element Resistance (ohms)

Serial Number: 93171-2

1	2	3	4	5	6	7	8	9	10	11	12	13	14	15	16	17	18
123.5	123.3	123.4	123.7	o/c	124.6	124.6	125.0	124.7	125.2	126.3	126.3	126.4	126.3	126.3	126.4	126.4	124.0

Row A

19	20	21	22	23	24	25	26	27	28	29	30	31	32	33	34	35	36
124.3	124.2	124.3	124.6	124.7	125.0	124.8	125.3	126.0	126.7	126.5	126.3	126.9	123.7	123.5	123.3	123.1	127.0

1	2	3	4	5	6	7	8	9	10	11	12	13	14	15	16	17	18	19	20	21	22	23	24	25	26	27	28	29	30	31	32	33	34	35	36

A

B

A

B

1	2	3	4	5	6	7	8	9	10	11	12	13	14	15	16	17	18
123.8	123.6	126.7	123.8	126.0	124.7	125.0	125.2	125.3	125.2	124.7	124.5	124.4	124.4	124.5	124.6	125.3	124.4

Row B

19	20	21	22	23	24	25	26	27	28	29	30	31	32	33	34	35	36
124.5	124.9	124.5	124.5	124.7	124.9	124.7	124.8	125.3	126.2	126.6	126.0	123.4	125.3	124.7	124.1	124.6	123.4

Test Officer...*[Signature]*

Date...*5/12/93*

85-115



2 x 36 INFRARED EMITTER ARRAY  
TEST DATA SHEET



Element Resistance (ohms) Serial Number: 93171- 5

1	2	3	4	5	6	7	8	9	10	11	12	13	14	15	16	17	18
118.9	119.1	119.2	120.1	120.1	120.3	120.3	120.6	120.5	120.4	120.1	120.2	120.2	120.0	119.7	119.7	119.7	119.5

Row A

19	20	21	22	23	24	25	26	27	28	29	30	31	32	33	34	35	36
120.0	117.8	119.6	120.1	120.4	119.7	120.0	120.4	120.5	120.7	119.9	119.0	117.4	118.5	118.7	118.3	118.3	118.4

B-22

1	2	3	4	5	6	7	8	9	10	11	12	13	14	15	16	17	18	19	20	21	22	23	24	25	26	27	28	29	30	31	32	33	34	35	36

A

B

A

B

1	2	3	4	5	6	7	8	9	10	11	12	13	14	15	16	17	18
116.7	118.8	120.9	119.2	119.5	120.0	120.1	121.5	120.8	123.7	120.4	120.1	120.2	120.1	120.0	120.0	120.3	119.8

Row B

19	20	21	22	23	24	25	26	27	28	29	30	31	32	33	34	35	36
117.7	120.0	117.8	119.8	120.0	117.8	120.0	117.7	120.5	120.0	120.2	120.6	117.9	121.2	118.7	118.1	120.6	118.0

Test Officer...*[Signature]*

Date...*6/12/93*

NS-49

# INITIAL DISTRIBUTION LIST

	<u>Copies</u>
IIT Research Institute ATTN: GACIAC 10 W. 35th Street Chicago, IL 60616	1
Naval Air Warfare Center Weapons Division, Code C2912 ATTN: Jim Bevan	1
Paul Amundson	1
B. J. Holden	1
Jim Ward	1
Dan Ommen	1
Jim Annos	1
China Lake, CA 93555	
46TW/TSWGI Guided Weapons Evaluation Facility 211 W. Eglin Parkway, Suite 128 ATTN: Buddy Goldsmith Eglin AFB, FL 32547	1
Naval Air Warfare Center Weapons Division Air Intercept System Department ATTN: Jerry Baker Pt. Mugu, CA 93042	1
WL/MNGI 101 W. Eglin Parkway, Suite 309 ATTN: Lee Murrer Eglin AFB, FL 32542	1
ARL/SLAD/EWD ATTN: AMSRL-SL-ES, Roy Gould Gary Johnson White Sands Missile Range, NM 88002	1 1
Army Research Laboratory ATTN: Martin Lahart Ft. Belvoir, VA 22060-5677	1
CECOM Center for Night Vision and EO AMSEL-SS-SE, Max Lorenzo Mike Lander Ft. Belvoir, VA 22060-5677	1 1

Copies

Air Force Test Flight Center  
412 Test Wing/TSDE  
195 South Popson Ave.  
ATTN: Keem B. Thiem  
Edwards AFB, CA 93524-6842

1

U. S. Army Research Office  
Physics Division  
P. O. Box 12211  
ATTN: Henry O. Everitt  
Research Triangle Park, NC 27709-2211

1

Naval Reseach Laboratory  
Code 5751  
ATTN: Paul Mark  
Washington, DC 20375-5000

1

Night Vision and Electro-Optic Sensors Dir.  
AMSEL-ED-NV-VISPD  
ATTN: Jerry Rusche  
Ft. Belvoir, VA 22060-5677

1

Naval Air Warfare Center  
Weapons Division, Code C2914  
ATTN: Jim Annos  
China Lake, CA 93555

1

Defense Nuclear Agency  
Simulation Technology Division  
HQ DNA/RAST  
ATTN: Andy Fahey  
6801 Telegraph Road  
Alexandria, VA 22310

1

Naval Air Warfare Center - Aircraft Division  
Building 2109/ATTN: SY04OS (David Blake)  
Patuxent River, MD 20670-5304

1

Arnold Engineering Development Center  
AEDC/DOTR  
ATTN: Mick Macklin  
Arnold AFB, TN 37389

1

		<u>Copies</u>
AMSMI-RD		1
AMSMI-RD-CS-R		15
AMSMI-RD-CS-T		1
AMSMI-RD-SS-HW,	Scott Mobley	3
	Alex Jolly	1
	James Buford	1
	Vicki Vanderford	25
AMSMI-GC-IP,	Mr. Fred Bush	1
STERT-TE-E-EO,	Eddie Burroughs	1